



## Novel Thermal Insulation in Future Building and District Heating Applications Hygrothermal Measurements and Analysis

AXEL BERGE

*Department of Civil and Environmental Engineering*  
*Division of Building Technology*  
CHALMERS UNIVERSITY OF TECHNOLOGY  
Gothenburg, Sweden, 2013



THESIS FOR THE DEGREE OF LICENTIATE OF ENGINEERING

# Novel Thermal Insulation in Future Building and District Heating Applications

Hygrothermal Measurements and Analysis

AXEL BERGE

Department of Civil and Environmental Engineering

CHALMERS UNIVERSITY OF TECHNOLOGY

Gothenburg, Sweden 2013

Novel Thermal Insulation in Future Building and District Heating Applications  
Hygrothermal Measurements and Analysis  
AXEL BERGE

© AXEL BERGE, 2013.

Lic / Department of Civil and Environmental Engineering  
Chalmers University of Technology  
Lic 2013:6  
ISSN 1652-9146

Department of Civil and Environmental Engineering  
Division of Building Technology  
Chalmers University of Technology  
SE-412 96 Göteborg  
Sweden  
Telephone + 46 (0)31-772 1000

Cover:  
Water drop on a hydrophobic aerogel blanket. The image reappears on page 7.  
(Photo: Axel Berge)

Chalmers Reproservice  
Göteborg, Sweden 2013

## Abstract

The interest for reducing the energy consumption in society has increased during the last decades due to an increased environmental awareness. One way to decrease the energy losses in the building sector is to improve the thermal insulation of building envelopes and installations and thereby decrease the heat losses.

This thesis analyzes two types of novel insulation with low thermal conductivity; aerogel blankets and vacuum insulation panels. The thesis aims to investigate the possible benefits from using these novel insulations, but also to evaluate new considerations related to the high insulation performance. The insulations have been tested in two applications:

1. A wooden stud wall with aerogel blankets as insulation
2. Hybrid insulated district heating pipes where aerogel blankets or vacuum insulation panels have been wrapped around the carrier pipe and polyurethane have been used to fill the rest of the casing pipe.

Thermal properties and moisture properties have been measured in laboratory by guarded heat flow meter, guarded hot pipe, transient plane source and wet cup method. District heating pipes with vacuum insulation panels have also been measured in field. The measured properties have been used in numerical simulations to evaluate the heat losses and the risk of moisture related damages for both applications.

The studies show promising results for aerogel blanket insulated walls where the wall thickness was reduced by 40 percent compared to a conventional Swedish wall. However, the effect on the moisture conditions from the thermal bridges through the studs has to be considered in order to avoid damages. For district heating pipes, the vacuum insulation panels showed the most promising results with a decrease in the heat losses by 15 to 25 percent depending on the dimensions of the pipe and the thickness of the vacuum insulation panels. In hybrid insulation double pipes with vacuum insulation, the position of the thermal bridges at the edges of the panel has a large impact on the total heat losses.

The thesis also examines some challenges when measuring the properties of the novel insulation. The thermal conductivity of aerogel blankets improves with an increased compression of the samples. The properties of the curved vacuum insulation panels used in the district heating pipes are difficult to measure since there is an impact from the thermal bridges along the edges, which might be influenced by surrounding materials.

Key words: aerogel blankets, vacuum insulation panels, district heating, wooden stud walls, superinsulation, thermal conductivity



## List of papers

The thesis is based on the following papers which are appended:

- I. Berge, A., Adl-Zarrabi, B. & Hagentoft, C. (2012) Determination of specific heat capacity by Transient Plane Source. *Proceedings of the 5<sup>th</sup> International Building Physics Conference*, Kyoto, Japan.
- II. Berge, A. & Adl-Zarrabi, B (2012) Using high performance insulation in district heating pipes. *Proceedings of 13<sup>th</sup> International Symposium on District Heating and Cooling*, Copenhagen, Denmark.
- III. Berge, A., Hagentoft, C. & Wahlgren, P. (2013) Wooden Stud Walls With Aerogel Thermal Insulation. Material Properties and HAM-Simulations. *Accepted for Buildings XII conference*, Clearwater, Florida, USA. Dec 1-5, 2013.

Paper I is written by me in collaboration with Bijan Adl-Zarrabi and Carl-Eric Hagentoft. The paper covers my work with a model for heat capacity measurements with a transient plane source sensor. I have performed the measurements, the analysis of the measured data and written the main part of the paper.

Paper II is written by me in collaboration with Bijan Adl-Zarrabi, based on our joint work with measurements on high performance insulation used in district heating pipes. I have made the guarded hot pipe measurements and the calculations of effective thermal conductivity and I have written the main part of the paper.

Paper III is written by me in collaboration with Carl-Eric Hagentoft, Paula Wahlgren and covers my measurements on aerogel blankets and heat and moisture simulations of a wooden stud wall with aerogel blanket insulation. I have made the measurements of thermal conductivity and vapor permeability, the simulations of the different walls. The main part of the paper was written by me.

The thesis is also based on two reports which are not appended:

- i. Berge, A. & Johansson, P. (2012) Literature Review of High Performance Thermal Insulation. Report 2012:2, Division of Building Technology, Chalmers University of Technology, Göteborg, Sweden.
- ii. Berge, A. & Adl-Zarrabi, B (2012) Högpresterande fjärrvärmerör [High performance district heating pipes], Report 2012:16, Fjärrsyn. (in Swedish)

Report i was written by me and Pär Johansson and is a literature review of the research field of high performance thermal insulation. The report have been written in equal parts by me and Pär Johansson.

Report ii is written by me and Bijan Adl-Zarrabi and is based on our joint research on district heating pipes with high performance insulation. The report covers laboratory measurements, field measurements and simulations. I have done the guarded hot pipe measurements, planned and executed the field measurements, made simulations of energy losses and analyzed measurement data. The report is written in equal parts by me and Bijan Adl-Zarrabi.



# Table of Contents

Abstract .....	i
List of papers .....	iii
Preface .....	vii
Notations and abbreviations .....	ix
1 Introduction.....	1
1.1 Heat transfer in nanoporous insulation.....	1
1.2 Aerogels.....	5
1.2.1 Properties of silica aerogel .....	7
1.2.2 Aerogel composites .....	8
1.2.3 Applications of aerogel insulation.....	9
1.3 Vacuum Insulation panels .....	10
1.3.1 Structure of vacuum insulation panels .....	10
1.3.2 Properties of vacuum insulation panels.....	11
1.3.3 Applications of vacuum insulated panels.....	12
2 Objectives .....	14
2.1 Aim .....	14
2.2 Scope and limitations.....	14
2.3 Method.....	15
3 Material properties and measurement methods .....	16
3.1 Guarded heat flow meter .....	16
3.2 Cup method.....	18
3.3 Transient Plane Source heat capacity measurements .....	19
4 Aerogel blanket wooden stud walls .....	22
5 Hybrid district heating pipes.....	26
5.1 Laboratory measurements.....	26
5.1.1 Guarded hot pipe .....	26
5.1.2 Field measurements preparations .....	28
5.2 Field measurements .....	30
5.3 Theoretical models .....	32
5.3.1 Description of numerical model.....	32
5.3.2 Network model for arbitrary boundary conditions.....	33
5.3.3 Calculation of heat losses.....	34

5.3.4	Optimization of thermal bridge position .....	35
6	Conclusion .....	38
7	Future studies .....	39
8	References.....	41

## Preface

This thesis summarizes the work during two years of studies at the division of Building Technology in the research group of Building Physics, Chalmers University of Technology.

The work has been financed through three different projects:

1. Homes 4 Tomorrow funded by FORMAS, the Swedish Research Council for Environment, Agricultural Sciences and Spatial Planning,
2. FC-District financed funded by EU.
3. Högpresterande fjärrvärmerör [High performance district heating pipes] a Fjärrsyn project funded by Swedish District Heating Association.

The work have been made possible with the help of Varberg Energi, Who have accepted to integrate district heating pipe prototypes into their district heating grid for field measurements, and Power Pipe, who have helped in the creation of prototypes for testing novel insulation in district heating pipes.

I want to thank all my colleagues at the division of Building Technology for a good working environment and stimulating discussions, especially my supervisors Carl-Eric Hagentoft, Paula Wahlgren and Bijan Adl-Zarrabi without whom I would be lost.

I would also like to thank my friends and family for their support and above all my wife Bonnie.

Axel Berge

Göteborg, May 2013



# Notations and abbreviations

## Roman uppercase letters

$K$	Thermal conductance	[W/K]
$Kn$	Knudsen number	[-]
$P$	Gas pressure	[Pa]
$T$	Temperature	[K][°C]

## Roman lowercase letters

$c_p$	Specific heat capacity	[J/(kg·K)]
$d$	Molecule diameter	[m]
$k_B$	$1.3806 \cdot 10^{-23}$ Boltzmann constant	[Pa·m <sup>3</sup> /K]
$l_{avg}$	Mean free path (m),	[m]
$q$	Heat flux	[W/m <sup>2</sup> ]
$t$	Time	[s]
$v$	Humidity by volume	[kg/m <sup>3</sup> ]
$v_s$	Saturation humidity by volume	[kg/m <sup>3</sup> ]

## Greek lowercase letters

$\beta$	Energy exchange factor	[-]
$\delta$	Characteristic system size	[m]
$\delta_p$	vapor permeability	[kg/Pa/s/m]
$\delta_v$	Vapor diffusivity	[m <sup>2</sup> /s]
$\lambda$	Thermal conductivity	[W/(m·K)]
$\zeta$	Moisture capacity	[kg/m <sup>3</sup> ]
$\rho$	Density	[kg/m <sup>3</sup> ]

## Index letters

$ext$	External
$g$	Gas
$g$	Ground
$i$	Insulation
$i+$	Superinsulation
$int$	Internal
$r$	Return
$s$	Supply
$v$	Vapor
$eff$	Effective

## **Abbreviations**

<i>d</i>	Down
<i>DN</i>	Nominal pipe diameter
<i>PUR</i>	Polyurethane
<i>R</i>	Return pipe
<i>s</i>	Side
<i>S</i>	Supply pipe
<i>u</i>	Up
<i>VIP</i>	Vacuum insulation panel

# 1 Introduction

The interest for reducing the energy consumption in society has increased during the last decades due to an increased environmental awareness.

Wherever two micro environments with different temperatures are separated, thermal energy will transfer from the higher temperature to the lower. The magnitude of the heat transfer is dependent on the properties of the insulation, the magnitude of the temperature difference and the area in between the environments. If the energy is transferred to a place where it isn't needed, for example the outdoor air, it is considered a loss.

In the building sector temperature differences are created for various purposes. Two examples which will be the focus of this report are:

- When the indoor temperature is held separate from the outdoor temperature to create a comfortable indoor climate, a temperature difference over the building envelope is created.
- High temperature fluids are used to distribute of thermal energy to places where the thermal energy is needed. These kinds of distribution systems have a temperature difference to the surrounding.

One way to decrease the heat losses is to use insulation with lower thermal conductivity. Insulation with a thermal conductivity below  $20 \text{ mW}/(\text{m}\cdot\text{K})$  is in this work referred to as superinsulation. Vacuum insulation panels and aerogel are two types of superinsulation with low thermal conductivity compared to conventional insulation such as mineral wool or extruded polystyrene. Berge & Johansson (2012) describes the properties of these materials and summarize the research in the area but a shortened summary will follow below. This thesis investigates how to evaluate the properties of these novel types of insulation, and further look at possible applications for the insulation.

## 1.1 Heat transfer in nanoporous insulation

The heat transfer through porous insulation materials is due to a combined process of heat conduction through pore walls as well as through the pore gas and long wave radiation between the pore surfaces.

Conventional insulation materials like mineral wool or expanded polystyrene use air as the main insulator. Still air has a very low thermal conductivity, but as soon as temperature gradients are created, the air can start to move, with the consequence that the heat transfer increases. This is called natural convection. Materials with a high porosity will mainly consist of air but if the pores are small enough the air cannot move and the convection transport will not start. This creates a lower limit for the thermal conductivity of conventional insulation, which is above the thermal conductivity of air, at  $26 \text{ mW}/(\text{m}\cdot\text{K})$ . Figure 1.1 shows the thermal conductivities of several insulation types, compared to the thermal conductivity of air.

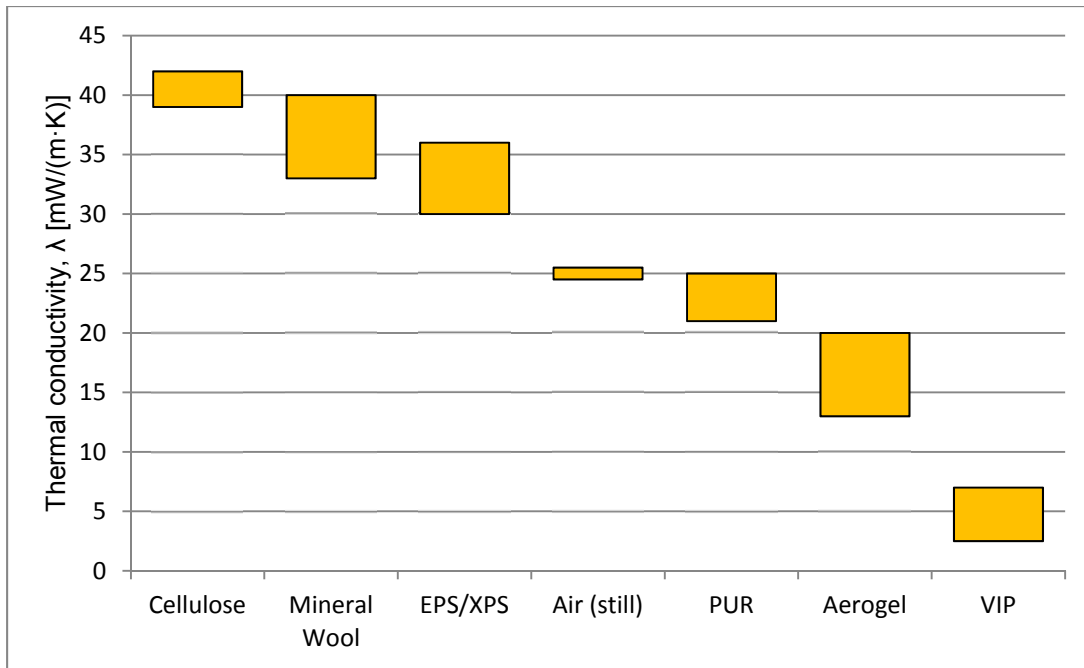


Figure 1.1 Approximate thermal conductivities for different insulation types and air at 10°C. Mainly from Petersson (2009).

To decrease the thermal conduction through the pore gas below that of air, as for the insulations to the right of the air bar in Figure 1.1, there are three main principles to work with:

1. If the cavities are filled with a gas with a lower thermal conductivity than air, that conductivity will be the lower limit instead. This principle is used in polyurethane and noble gas filled windows.
2. With the gas removed altogether there cannot be any gas conduction. This principle is used in thermos bottles and in vacuum insulation panels.
3. Small pores with a size below the mean free path decrease the collisions between air molecules. This principle is used in aerogels and is also an important property for vacuum insulation panels.

The last two points are connected and that is why both principles exist in vacuum insulation, which will be explained later in this chapter. On the other hand both two last principles counteract the first principle since they lower the influence of the gas conduction.

Collisions between two gas molecules transfer much more energy than the collision between a gas molecule and a solid structure. This means that if the rate of collisions between gas molecules is reduced, the thermal conduction through the gas will also reduce. This leads to the definition of an important term; the mean free path. The mean free path of a gas is defined as the average distance a gas molecule have to travel before colliding with another gas molecule and it can be calculated by Equation (1).

$$l_{avg} = \frac{k_B T}{\sqrt{2} \pi d^2 P_g} \quad (1)$$

where  $l_{avg}$  is the mean free path (m),  $k_B$  is the Boltzmann constant ( $\text{Pa} \cdot \text{m}^3/\text{K}$ ),  $T$  is the temperature (K),  $d$  is the molecule diameter (m) and  $P_g$  is the gas pressure (Pa).

For a pore system where the pore size is around or lower than the mean free path, the probability for gas to gas collisions will decrease in favor for collisions with the pore walls. This will thus lower the thermal conduction through the gas in a simplified system by Equation (2). This is called the Knudsen effect and is governed by the Knudsen number, shown in Equation (3).

$$\lambda_g = \frac{\lambda_{g,0}}{1 + 2\beta Kn} \quad (2)$$

where  $\lambda_g$  is the gas conductivity in limited spaces ( $\text{W}/(\text{m} \cdot \text{K})$ ),  $\lambda_{g,0}$  is the gas conductivity for still gas ( $\text{W}/(\text{m} \cdot \text{K})$ ),  $\beta$  is a constant correlated to the magnitude of the energy exchange between the gas and the solid walls (-) which has a value between 1.5 and 2 (Baetens et al., 2010) and  $Kn$  is the Knudsen number (-) calculated by Equation (3):

$$Kn = \frac{l_{avg}}{\delta} \quad (3)$$

where  $\delta$  is the characteristic system size (m). The distance  $\delta$  is correlated to the pore size but does not represent any average pore dimension. The characteristic system size corresponds to a setup with two parallel plane surfaces at a distance  $\delta$  from each other. This means that this model cannot be used to calculate the actual gas conductivity for a nanoporous material but it can be used to show the principals of the physics and to show size magnitudes for the effect to appear.

The conductivity of air as a function of characteristic system size is shown in Figure 1.2. The conductivities have been calculated for a temperature of  $20^\circ\text{C}$ , atmospheric pressure at 100 kPa and an energy exchange factor,  $\beta$  in Equation (2), of 1.75. For air the mean free path is around 100 nm and a characteristic pore size around 100 nm shows a fast change in the thermal conductivity.

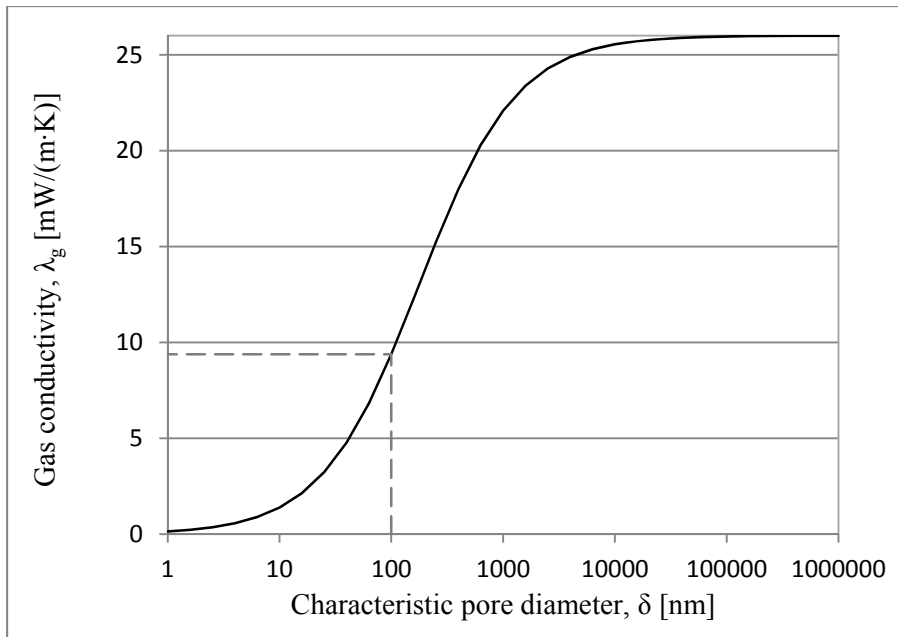


*Figure 1.2 Gas conductivity in a porous material as a function of the characteristic pore size at 20°C and a pressure of 100 kPa for a heat exchange constant of 1.75. The mean free path of air is 100 nm which is marked with the dashed line.*

As shown in Equation (1), the mean free path is dependent of pressure. For a lower pressure, the mean free path increases and thus the thermal conductivity decreases. This is seen in Figure 1.3 which shows the gas conductivity as a function of gas pressure for a variation of characteristic system sizes. For a smaller system size a higher pressure can still eliminate the influence from gas conduction in the heat transfer. This means that an evacuated nanoporous material can withstand a larger accumulation of gas before the conductivity starts to increase. This leads to an increased service life for evacuated insulation with a nanoporous core.

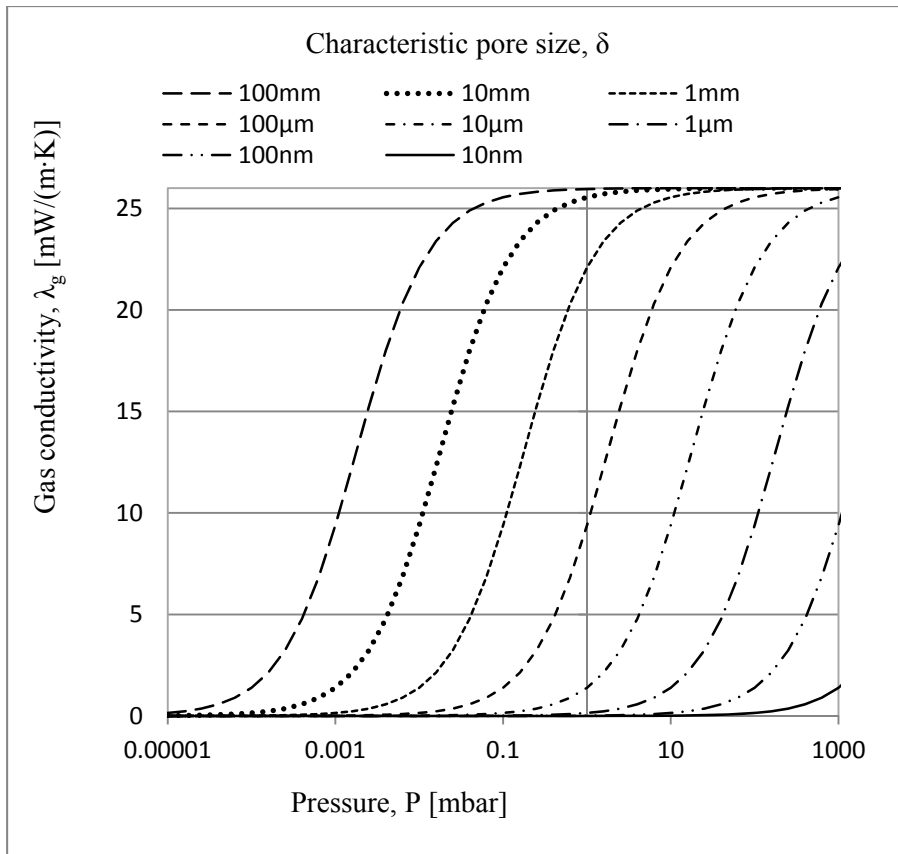


Figure 1.3 Gas conductivity in a porous material as a function of internal pressure for various characteristic pore sizes.

## 1.2 Aerogels

Aerogels are former gels which have been dried in such a way that the structure of the solid in the gel is preserved. Pure silica aerogel is created in two forms; as monolithic blocks of continuous aerogel and as aerogel granulates, shown in Figure 1.4. For opacified aerogels, the thermal conductivity is as low as 13 mW/(m·K) (Fricke et al., 1991) which is close to half of the conductivity of still air.

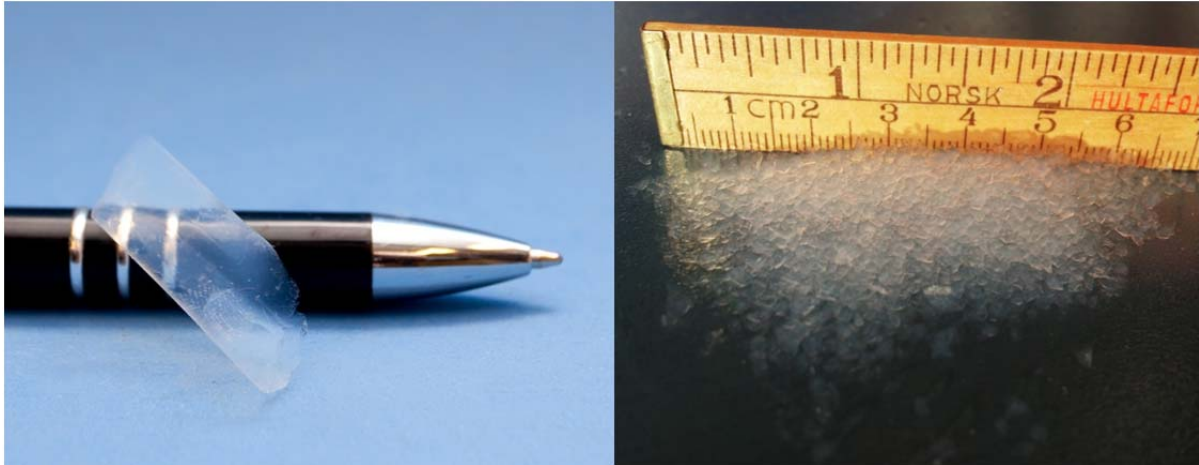


Figure 1.4 The left image shows a piece of monolithic aerogel and the right image shows aerogel granulates.  
 (Left photo: Nina Zanders) (Right photo: Axel Berge)

The concept was first examined by Kistler (1931) who realized that the shrinkage of drying gels was the consequence of the gel structure collapsing because of forces created when the liquid in the pores evaporated. Kistler (1931) showed that those forces could be eliminated by exchanging the pore liquid with a gas at a pressure and temperature above the critical point, shown in Figure 1.5. If the combined temperature and pressure is raised along the line between point 1 and 2, a supercritical state is reached without any transition from liquid to gas.

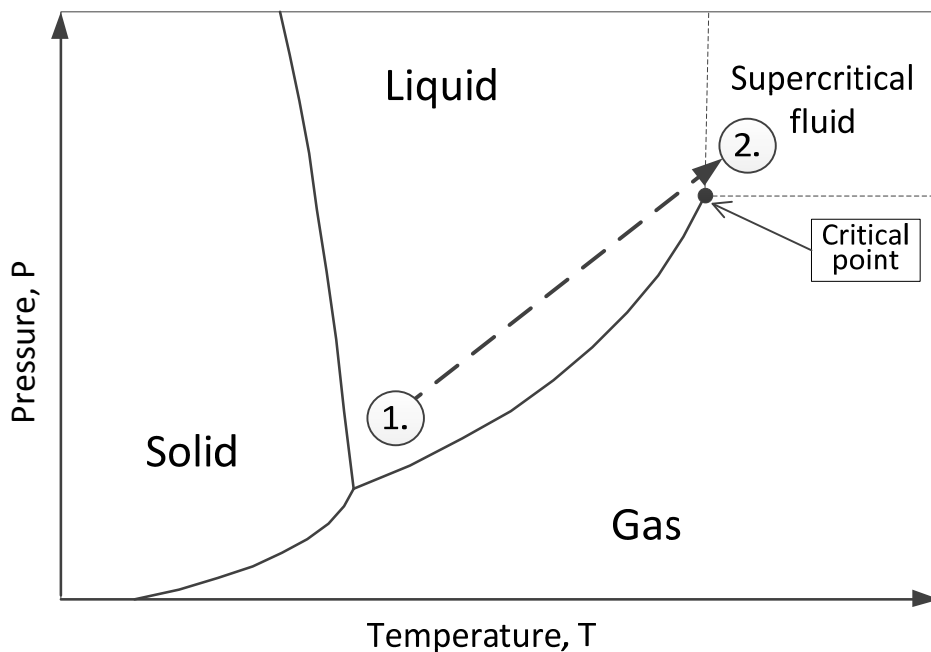


Figure 1.5 Principle image of a phase diagram. If the pressure and temperature is raised along the line between 1 and 2, the material is liquid all the time. At 2, above the critical point, the liquid can be exchanged with a gas without creating tensile forces.

Aerogel can be created from a wide variety of gels based on for example organic molecules, silicates or various metal oxides. For insulation applications, the most common type is silica aerogels because of a low cost and a developed production procedure. Silica aerogels will thus be the focus of this chapter but other types of aerogel could be interesting due to various other properties.

### 1.2.1 Properties of silica aerogel

Fricke et al. (1991) measured the thermal conductivity for opacified monolithic silica aerogel of various different densities and different amount of opacifier. The results led to a model for the proportionality between density and the various modes of heat transfer, a higher density increase the conduction through the solid gel structure while the gas conduction and the radiation decrease. Fricke et al. (1991) found a minimum thermal conductivity at 13 mW/(m·K) for an aerogel with a density of 120 kg/m<sup>3</sup> and an addition of 5% soot to the gel. Hümmer et al. (1993) continued the work and tested the thermal conductivity of opaque aerogels ground to granulates or powder which was found to have a higher thermal conductivity, above 20mW/(m·K).

In its pure form, silica aerogel is transparent. Nilsson et al. (1985) measured a thermal conductivity of 17 mW/(m·K) on a transparent silica aerogel but their measurement method used a low emissivity hot strip which would decrease the heat transfer from radiation. Rubin et al. (1983) measured the thermal properties of transparent silica aerogel in relation to the solar transmittance. Their aerogel had a thermal conductivity 19 mW/(m·K). The windows showed similar U-values to double or triple windows with the same transmittance.

While silica aerogel, optimized for low thermal conductivity, have a density around 100 kg/m<sup>3</sup> Tillotson et al. (1992) managed to create an aerogel with a density of 3 kg/m<sup>3</sup>. Tamon et al. (1997) measured the pore distribution with a N<sub>2</sub> adsorption method for various aerogels with a density around 200 kg/m<sup>3</sup> and to a porosity around 80%. The pore size is distributed in between 1 nm and 100 nm with a high peak around 10 nm. This indicate a porosity of around 90% for a silica aerogel with a density at 100 kg/m<sup>3</sup>.

The high porosity in combination with small pores gives a large surface area which gives a risk of adsorbing large amounts of water in the hygroscopic range. To avoid this problem the aerogel can be chemically engineered to be hydrophobic. This will lower the accumulation of water in the material which otherwise could destroy the structure when dried. The hydrophobicity of an aerogel composite is shown in Figure 1.6 where it is seen that the drops become almost spherical.



*Figure 1.6 Water drop on a hydrophobic aerogel blanket. (Photo: Axel Berge)*

One of the main drawbacks of silica aerogel is its fragility. Parmenter and Milsten (1998) tested the mechanical properties of aerogel and found the compressive strength to be around 1 MPa and the shear strength around 0.1 MPa. This gives incentives to reinforce the aerogel to decrease the fragility.

### **1.2.2 Aerogel composites**

To adapt silica aerogel insulation to various types of applications some composites have been created where the aerogel is mixed with other materials.

Stahl et al. (2012) have created an insulation rendering consisting of silica aerogel granulates blended with a mineral binder. The rendering has a thermal conductivity of 25 mW/(m·K) and can be applied in layers with a thickness around 6 cm. The rendering can be used to enhance the thermal performance of retrofitted rendered buildings with a cultural historic value.

Another aerogel composite is the aerogel blanket, shown in Figure 1.7. By gelating aerogel in a lofty polymer batting, a flexible blanket is created. The blankets contain a monolithic aerogel which is held together by the reinforcing batting. Pietruska et al. (2012) analyzed various blankets and measured their thermal conductivity to 15-16 mW/(m·K) and their vapor permeability to around 0.02 g/(m·h·hPa) which corresponds to  $7.4 \cdot 10^{-6}$  m<sup>2</sup>/s. The blankets are hydrophobic but Pietruska et al. (2012) shows that they can be filled with water by immersion which then can create frost damage on the structure if exposed to freeze thaw cycles.



*Figure 1.7 A roll of aerogel blanket. (Photo: Nina Zanders)*

### **1.2.3 Applications of aerogel insulation**

Most examples of application of aerogel have been commercial and have not been published in scientific journals. Some examples are although put forward by various product producers.

Aerogel blankets have been used as both interior and exterior insulation. For a building where several layers of aerogel blankets were mounted on both sides of the wall, the U-value was decreased from 1 to 0.2 W/(m<sup>2</sup>·K) (ASPEN, 2011a). In another building, the flexibility of the aerogel blankets was used to insulate a vaulted roof with minimal decrease of the roof height.

Aerogel blankets can be used to eliminate or decrease the impact of thermal bridges. Pietruszka & Gerylo (2010) calculated the effect of using low conductivity insulation, using thermal conductivities obtained for aerogel blankets, in the frames of curtain walls. They concluded that a low thermal conductivity is needed in the frame insulation to be able to make an impact on the total U-value of the curtain wall. ASPEN (2012d) used stripes of aerogel blankets glued onto the studs in a wooden stud wall to increase the thermal resistance of the wall with 15%. ASPEN (2012c) also shows an example of usage for aerogel blankets in the thin space behind a box for window blinds. The box was placed in line with the exterior wall surface where it replaced some of the insulation through the wall.

STOAKES (2012) retail a daylight solution in the form of curtain walls filled with transparent aerogel granulates. The U-value is specified to 0.28 W/(m<sup>2</sup>·K) for walls with a light transmittance of 13%. This can be compared to Reim et al. (2005) who created a similar construction with U-values in between 0.37 W/(m<sup>2</sup>·K) and 0.47 W/(m<sup>2</sup>·K) with a corresponding solar transmittance in between 19% and 54% where the gas in the aerogel was exchanged with noble gas.

### 1.3 Vacuum Insulation panels

Vacuum insulation panels are a novel type of insulation consisting of an evacuated porous core material enveloped by a material with low air permeation. The vacuum inside the panels decreases the thermal conductivity through the gas, which gives a thermal conductivity as low as  $2.5 \text{ mW}/(\text{m}\cdot\text{K})$  in the center of the panel, depending on the choice of material.

Figure 1.8 shows two vacuum insulation panels; one flat panel, which is the common type used as building wall insulation, and a curved panel which can be used as insulation around pipes or columns.



*Figure 1.8 Two vacuum panels, to the left is a flat vacuum panel fitting as wall insulation and to the right is a curved insulation panel for use around pipes or columns. (Photo: Axel Berge)*

#### 1.3.1 Structure of vacuum insulation panels

Vacuum insulation panels commonly consist of an evacuated porous core material encapsulated in a multi-layered metalized laminate. A cut up panel is shown in Figure 1.9 which also shows a layer of protective cloth wrapped around the core material to hold it together and keep the shape.

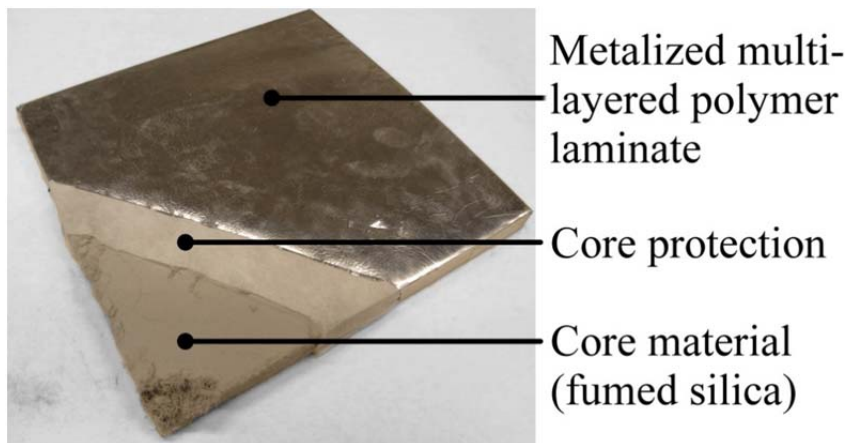


*Figure 1.9 A vacuum insulation panel, cut open to show the different layers.  
(Photo: Axel Berge)*

The core material can be of various types which gives different benefits. All core materials have to have some common properties; they must be porous to be able to be evacuated and they have to be able to withstand the pressure from the ambient air without losing its shape.

Around the core material is a metalized multi-layered polymer laminate, built by alternating layers of polymers and aluminum. Its purpose is to hinder the permeation of air into the vacuum panels and thus keep the vacuum at a low level as long as possible. Thicker layers of aluminum decrease the permeation but it also creates a thermal bridge along the edges of the panel which will degrade the thermal performance of the whole panel.

### **1.3.2 Properties of vacuum insulation panels**

The thermal conductivity of vacuum insulation panels depends on the choice of core material. Heinemann (2005) shows measured thermal conductivities as a function of pressure for various porous materials. The lowest thermal conductivity, around  $2.5 \text{ mW}/(\text{m}\cdot\text{K})$ , is measured for glass fibers but the thermal conductivity starts to increase already at 0.1 mbar due to the large pore size. Fumed silica gives a higher thermal conductivity, a minimum around  $4 \text{ mW}/(\text{m}\cdot\text{K})$ , but the thermal conductivity doesn't increase significantly until the pressure reaches around 10 mbar. This gives fumed silica a longer lifespan, even though glass fibers can give a lower thermal conductivity at an early stage. Therefore, fumed silica is more appropriate as a core material for building applications, where the expected life span is decades.

Simmler et al. (2005) tested the temperature dependence of the thermal conductivity of fumed silica vacuum panels. The thermal conductivity raised by around  $2 \text{ mW}/(\text{m}\cdot\text{K})$  from  $3.5 \text{ mW}/(\text{m}\cdot\text{K})$  to  $5.5 \text{ mW}/(\text{m}\cdot\text{K})$  in between  $0^\circ\text{C}$  and  $100^\circ\text{C}$ . Even at as high temperatures as  $100^\circ\text{C}$ , vacuum insulation panels still have a very low thermal conductivity.

The life time performance of the vacuum insulation panels depend on the permeation of gases through the metalized laminate. The laminate is typically constructed of alternating layers of polymers and aluminum. Some examples are shown by Baetens et al. (2010) and their calculated age deterioration shows that more or thicker aluminum layers lower the overall permeation through the laminate, and thus prolong the life time of the panel.

At high temperatures the permeation rate increases. Simmler & Brunner (2005) show an exponential relation between the pressure increment rate and the temperature. This means that it gets even more important with a low permeation for high temperature applications. High temperatures do also create a demand for a higher melting point in the sealing layer of the metalized laminates. Different polymers were tested by Araki et al. (2009) who show that commonly used laminates were improper for high temperature applications but that there were other possible materials which could increase the high temperature permeation performance of the metalized laminates.

As mentioned, the permeation rate decreases with more aluminum and the life time increase. At the same time, the aluminum has a very high thermal conductivity, which creates thermal bridges along the edges of the vacuum insulation panels. IN addition, more aluminum creates a larger impact from the thermal bridges. Binz et al. (2005) have made estimations of the effective thermal conductivity of a vacuum insulation panel with the dimensions 1.00 x 0.50 x 0.02 m<sup>3</sup> with a center of panel thermal conductivity of 4 mW/(m·K). The effective conductivity was 8.6 mW/(m·K) with an 8 μm aluminum foil and 5.1 mW/(m·K) with a three layer metalized laminate. This means that the increase in the center of panel thermal conductivity was 115 percent and 28 percent respectively.

To preserve the low thermal conductivity in the vacuum panels it is important to keep the low internal pressure. A single damage to the permeation tight barrier might ruin the vacuum and thus ruin the thermal performance. Therefore, vacuum insulation panels demand extra caution when installed in their specific application, compared to other insulation materials.

The vulnerability and stiffness of the vacuum insulation panels makes them impossible to change to fit at the workplace or adapt to uneven surfaces. The panels can be created to fit certain non-flat forms, an example of the method is shown in Figure 1.10, but the shape has to be predetermined when the panels are ordered.

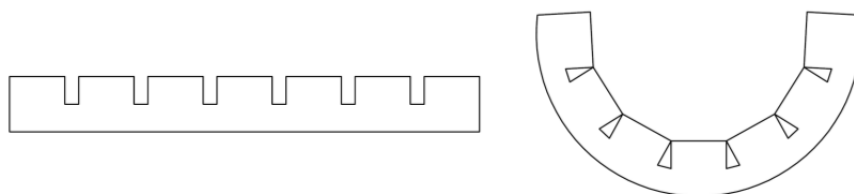


*Figure 1.10 Example of a cylindrical vacuum insulation panel. Indentations in the core material bend the panel when it is evacuated so that it can fit around a cylindrical geometry.*

### **1.3.3 Applications of vacuum insulated panels**

Vacuum insulation panels have been used in various types of applications such as refrigerators and thermo stable packaging (Va-q-tec, 2013). The work in IEA/ECBCS-Annex 39 collects several examples of applications for vacuum insulation panels in Binz et al. (2005). Eriksson (2012) have made a study on high performance insulation and possible applications in the Swedish building stock. Information about various building projects using vacuum insulation panels can also be found at Vip-bau (2013).

Johansson (2012) has written a review of building applications for vacuum insulation panels and concludes that one of the most beneficial usages is for places where the thickness is limited. For roof terraces there is often an ambition to make the indoor and outdoor floor at the same height. This creates a limitation to the thickness of the terrace insulation. Simmler & Brunner (2008) makes in-situ measurements on a flat roof construction and concludes that the ageing effects cannot be neglected and has to be considered during the design. The vacuum insulation panels can be working for decades, but proper values for the thermal performance, representing average properties during the panels' life time, must be used in the design.

When retrofitting old buildings cultural heritage considerations might have to be taken. This can limit the possibilities to add thick amounts of insulation to the façade. With vacuum insulation panels, a thinner solution is possible. An example is shown by Johansson (2012) who made measurements on an old wooden façade building with a combination of vacuum insulation panels and mineral wool added behind the façade. The U-value of the walls was reduced from  $1.11 \text{ W}/(\text{m}^2 \cdot \text{K})$  to  $0.40 \text{ W}/(\text{m}^2 \cdot \text{K})$  with an additional thickness of 50 mm. Sveipe et al. (2011) made humidity measurements in a climate chamber of various retrofit solutions using vacuum insulation on wooden stud walls with 100 mm mineral wool insulation. Simulations of their best performing solution, with an addition of 30 mm vacuum insulation panels on the outside of the original wall, lowered the U-value from  $0.411 \text{ W}/(\text{m}^2 \cdot \text{K})$  to  $0.143 \text{ W}/(\text{m}^2 \cdot \text{K})$ .

Haavi et al. (2012) measured the U-value of vacuum insulation panels in new wooden stud walls in a hot box. The best performing layout gave a U-value of 0.09 with a thickness of 182 mm, not considering any façade.

Kubina (2010) shows an example of vacuum insulation panels integrated in insulation foam. The foam protects the vacuum insulation panels from damage to make them easier to handle on a building site. The insulation system can be used both for retrofitting and in new buildings.

Fuchsa et al. (2012) investigated the possibilities of using vacuum insulation panels to insulate thermal storage units. He compares the volume of stored hot water to the volume of insulation and shows that the insulation takes up an important part of the volume for small heat storage tanks. For these, vacuum insulation would lead to large relative space savings.

## **2 Objectives**

### **2.1 Aim**

The aim of this thesis is to investigate properties and possibilities of novel insulation systems with low thermal conductivity. The work examines the challenges with the new insulation materials, both regarding consequences of their combination of properties and problems related to measuring these properties. The research questions in this thesis are:

Is novel insulation, like aerogel and vacuum insulation panels, applicable for building and district heating applications?

What kind of new effects appear, which have to be considered, when using these novel insulations?

What kind of benefits can be achieved by the use of novel insulation in new building constructions or district heating pipes?

Are today's methods for measurement of thermal properties appropriate for superinsulation?

### **2.2 Scope and limitations**

This thesis focuses on two types of novel insulation; aerogel blankets and fumed silica vacuum insulation panels. Both types have a very low thermal conductivity compared to conventional insulation and are already produced in large quantities. The tested materials are already commercially available with a specific chemical composition and thereby various pre-set properties.

The work has consisted of measurements of various properties related to heat and moisture transport. The measured data have been used to analyze district heating applications, for both aerogel blankets and vacuum insulation panels, and as wooden stud wall insulation, for aerogel blankets.

This study does not consider mechanical properties of the novel insulation. The durability of the insulation is discussed but not evaluated.

## **2.3 Method**

In order to analyze the properties of the insulations they have been tested in a variety of ways. Thermal properties have been measured with guarded heat flow meter and transient plane source. Moisture transport properties have been measured with wet cup method. The results have been used as input in calculations. The properties of larger structures have also been measured with guarded hot pipe, in an attempt to find appropriate calculation assumptions and to obtain some apparent material properties for composite material.

Field measurements of district heating pipes have been performed where the temperature in various positions in the pipes have been monitored continuously. The result has been used to draw some primary conclusions about the impact from using novel insulation in a real situation.

Numerical models have been built in the softwares Matlab, Comsol and WUFI 2D, which have been used to simulate various situations. The models have been used to analyze possible gains from novel insulation but also to find risks with the applications.

### 3 Material properties and measurement methods

To make hygrothermal models of insulation materials, some various material properties must be known. For heat, the transport is governed by the differential equation shown in Equation (4) together with Fourier's law shown in Equation (5). (Hagentoft, 2001)

$$\rho c_p \cdot \frac{\partial T}{\partial t} = -\nabla \cdot \mathbf{q} \quad (4)$$

$$\mathbf{q} = -\lambda \nabla T \quad (5)$$

where  $\rho$  is the density ( $\text{kg/m}^3$ ),  $c_p$  is the specific heat capacity at constant pressure ( $\text{J}/(\text{kg}\cdot\text{K})$ ),  $T$  is the temperature ( $\text{K}$ ),  $t$  is the time ( $\text{s}$ ),  $\mathbf{q}$  is the heat flow vector ( $\text{W}/\text{m}^2$ ) and  $\lambda$  is the thermal conductivity ( $\text{W}/(\text{m}\cdot\text{K})$ ).

The transport of moisture in a material by diffusion is governed Equation (6). (Hagentoft, 2001)

$$\mathbf{g} = -\delta_v \nabla v \quad (6)$$

where  $g$  is the moisture flux vector ( $\text{kg}/\text{m}^3$ ),  $\delta_v$  is the vapor permeability ( $\text{m}^2/\text{s}$ ) and  $v$  is the humidity by volume ( $\text{kg}/\text{m}^3$ ).

#### 3.1 Guarded heat flow meter

A guarded heat flow meter measures the heat flow through a sample in between two plates with constant temperatures. The meter is considered guarded since the constant temperature plates and the sample extend outside of the measurement zone. In that way, the heat flow can be assumed to be one dimensional. Thus, Fourier's law, shown in Equation (5), can be used to calculate the thermal conductivity since the temperature on both the sides, the heat flow and the sample thickness are known.

Macro scale heat radiation between the constant temperature boundaries will affect the heat transfer if the measured material is transparent for relevant wave lengths. This effect would show a variable thermal conductivity based on the thickness of the sample, and is called thickness effect.

In appended **Paper III**, the guarded heat flow meter was used to measure the thermal conductivity of aerogel blankets. The measurements were made on three layers of aerogel blanket with a nominal thickness of 10 mm. The results, as a function of temperature, are shown in Figure 3.1. The thermal conductivity at 10 °C was found to be around 15.3  $\text{mW}/(\text{m}\cdot\text{K})$  and increases with 0.02  $\text{mW}/(\text{m}\cdot\text{K})$  per °C.

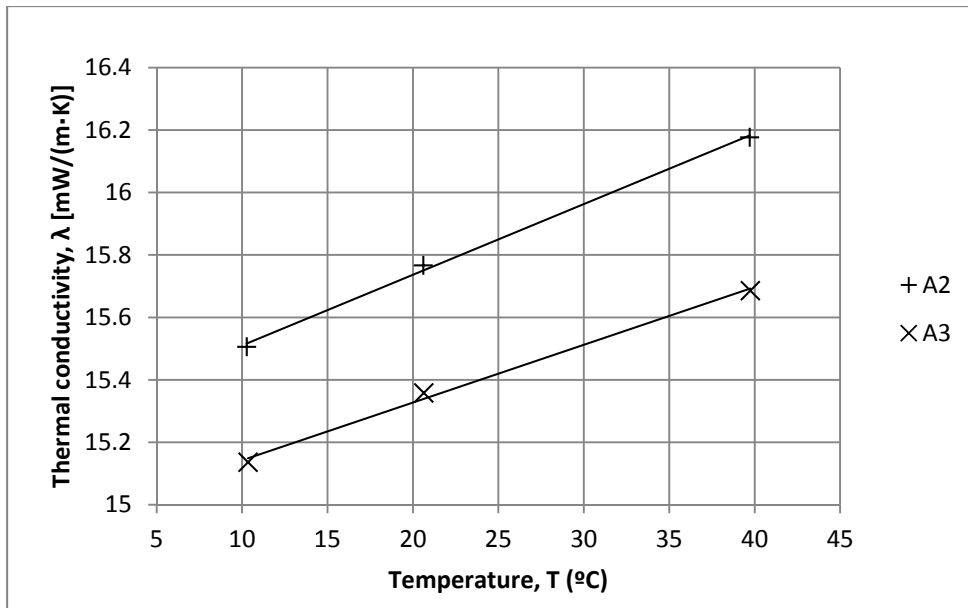


Figure 3.1 Thermal conductivity as a function of temperature, measured for two samples of aerogel blanket.

The thermal conductivity of aerogel blankets will also depend on the compression of the samples. Aerogel is a fragile material and in the aerogel blankets the aerogel is held together by fibers. Close to the surface, the aerogel deteriorate, why the surface layer consists of larger pores. The thermal conductivity of aerogel is less than for still air. If the surface layer with more air is compressed, the thermal conductivity of the sample would decrease. The dependency of compression was tested by varying thickness for three different samples. The results are shown in Figure 3.2 where a compressed sample gets a lower thermal conductivity than an uncompressed sample. It is although important to mention that the overall thermal transport through the sample increases, because of the reduced thickness, which can be seen in the increasing thermal conductance in Figure 3.2.

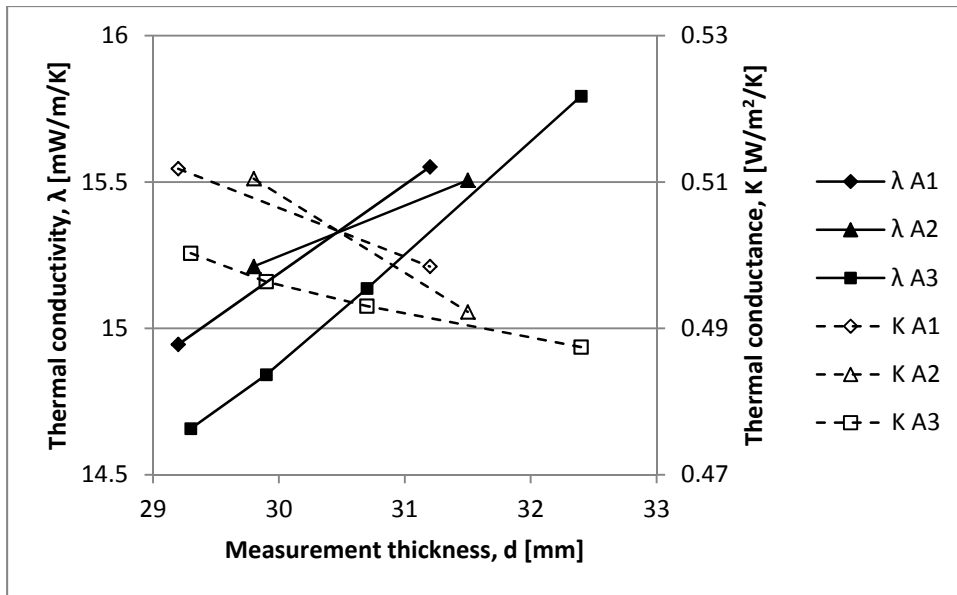


Figure 3.2 Thermal conductivity as a function of measurement thickness. The measurement thickness corresponds to various compressions of the samples. The solid lines show the thermal conductivity of the samples and the dashed lines show the thermal conductance through the samples.

### 3.2 Cup method

The wet cup method is used to measure the vapor permeability of materials. A sample is placed on top of a glass cup with water. The sample is sealed on the sides to create a one dimensional flow. The relative humidity at the water surface is 100 percent and the set-up is placed in a room with a constant relative humidity.

The vapor permeability of aerogel blankets were measured in **Paper III**. The dusty surface of the aerogel blankets makes a tight sealing difficult. Therefore, the blankets were tested for two different sizes. In that way, an increased moisture flow through the perimeter could be found and adjusted for. The results are shown in Table 3.1. The difference in between the two sizes is smaller than the difference between each measurement so the vapor flow through the perimeter seems to create a small variation compared to other factors. The large variation between similar samples could come from inhomogeneity in the material or because of aerogel particles falling of the surface during sample preparation.

Table 3.1 also shows the results for an aerogel blanket covered with a dust protection coating. The coated and uncoated samples have similar vapor permeabilities which show that the used coating can be applied without any large impact.

Table 3.1 Measurement of permeability on small and large samples of aerogel blanket, without (A) and with (B) a dust coating.

Sample	Vapor permeability, $\delta_v$ ( $\cdot 10^{-6} \text{ m}^2/\text{s}$ )	Vapor permeability, $\delta_p$ ( $\cdot 10^{-12} \text{ kg/Pa/s/m}$ )
A1 small	5.93	45
A2 small	5.54	42
A3 small	5.12	38
A <sub>avg</sub> small	5.53	42
A4 large	5.32	40
A5 large	5.15	39
A6 large	5.67	43
A <sub>avg</sub> large	5.38	40
A <sub>tot.avg</sub>	5.46	41
B1 large	6.32	48
B2 large	6.61	50
B3 large	5.78	43
B <sub>avg</sub>	6.24	47

### 3.3 Transient Plane Source heat capacity measurements

The heat capacity determines a materials ability to store thermal energy. Transient Plane Source is a method to measure thermal properties by analyzing the temperature development in a sensor which also works as a heat source with constant power input. A standard measurement with Transient Plane Source gives the thermal conductivity and the thermal diffusivity. From these, the heat capacity can be calculated.

For measurements of the diffusivity on anisotropic materials, the heat capacity is also needed as input data. **Paper I** examines a new method to measure the heat capacity with the help of Transient Heat Source equipment. In that way, only one set of equipment is needed for a wider variety of measurements.

The method is described in **Paper I**, where the Transient Plane Source sensor is attached to a sample container of gold, shown to the right in Figure 3.3 . The container and the sample are inserted into a steel cylinder, shown to the left in Figure 3.3, to create linear thermal losses from the system assuming that the steel surface is large enough compared to the cylinder to have a constant temperature during the short time span and small temperature gradients in the measurement.



Figure 3.3 The equipment used for heat capacity measurements. To the right is the sensor, glued to a golden sample container and to the left is the steel tube, which can be evacuated, into which the sensor and the sample is inserted. (Photo: Axel Berge)

To be able to calculate the heat capacity of a measured sample, a lumped model was created. The model estimates the heat transfer through the set-up, both with and without a sample, as shown in Figure 3.4.

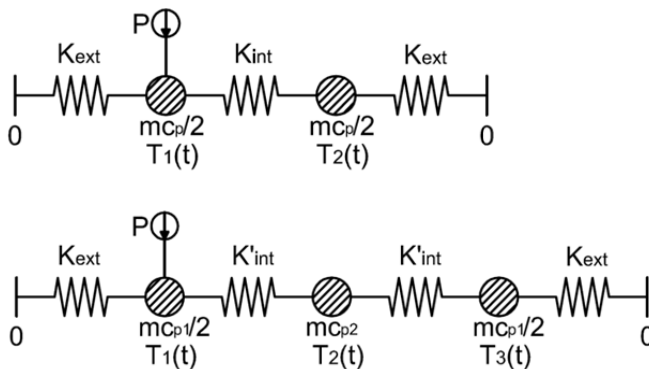


Figure 3.4 Thermal networks for the heat capacity model, for the case without a sample above and for the case with a sample below. Both the nodes in the network above and the outer nodes in the network below represent the two sides of the sample container. The middle node in the network below represent the sample.

The model for the case without the sample was solved analytically as expressed in Equation (7), Equation (8) and Equation (9). After some time, the influence from the term containing the internal conductance will decrease and the curve will only depend on the external

conductance and the heat capacity. These can then be obtained from a curve fit of the analytical solution to a measured curve for the case without any sample. The resulting external conductance and heat capacity can then be used as input for the analysis of the case with a sample defined by the lower network in Figure 3.4.

$$\begin{cases} T_1(t) = T_{s1} - \frac{T_{s1} + T_{s2}}{2} e^{-t/t_c} - \frac{T_{s1} - T_{s2}}{2} e^{-t/t'_c} \\ T_2(t) = T_{s2} - \frac{T_{s1} + T_{s2}}{2} e^{-t/t_c} + \frac{T_{s1} - T_{s2}}{2} e^{-t/t'_c} \end{cases} \quad (7)$$

$$t_c = \frac{mc_p}{2K_{ext}} \quad (8)$$

$$t'_c = \frac{mc_p}{2(K_{ext} + 2K_{int})} \quad (9)$$

where  $T_{s1}$  and  $T_{s2}$  are the steady state temperatures at corresponding node (K),  $t_c$  and  $t'_c$  is time constants (s),  $K_{ext}$  is the external conductances to the exterior (W/K) and  $K_{int}$  is the internal conductance from one side of the container to the other (W/K).

The network for the case with a sample was simulated for a variety of different internal conductances,  $K'_{int}$ , and sample heat capacities,  $mC_{p2}$ , and the results were fitted to the results from a measurement on a silver sample. The simulations underestimated the heat capacity of the silver sample by 6-8%.

The underestimation could be because of non-linear heat transfer. If the heat transfer increase with temperature, a linear model would interpret it as a lower heat capacity. Typical non-linear heat transfer could come from convection. An error could also come from the simplifications of the lumped model. The heat flow between the sides of the container is assumed to go through the sample, but some of the flow will go through the sides of the container.

## 4 Aerogel blanket wooden stud walls

**Paper III** evaluates the possible benefits of using aerogel blankets in wooden stud walls, some various wall assemblies were simulated numerically for thermal performance and moisture performance. The results were compared to walls with the same U-value but with conventional insulation. The main questions of interest have been the possible decrease in thickness from the use of aerogel blankets and finding possible moisture risks that can be created by the thinner walls.

The walls were based on a conventional solution for a low energy house with mineral wool insulation. The conventional walls were compared to walls with the same U-value but with the mineral wool exchanged with aerogel blankets. All walls had at least one homogenous material layer for which the thickness was adjusted until the U-value was exactly  $0.100 \text{ W/m}^2/\text{K}$ . The walls are shown in Figure 4.1. Wall 1a and 2 a are two types of the conventional Swedish walls with a variation of the position of the wooden studs and wall 2a, 2b, 3a and 3b is different variations of aerogel walls.

The walls consist of the following elements with material data found in **paper III**:

1. 13 mm gypsum board
2. 45 mm service penetration layer with insulation and wooden studs
3. Vapor tight film
4. Homogeneous layer of insulation, H1, for walls 1 and 2
5. The load bearing part of the wall with insulation and wooden studs
6. Homogeneous layer of insulation, H2, for walls 1 and 3
7. 25 mm ventilated air gap
8. Wooden façade

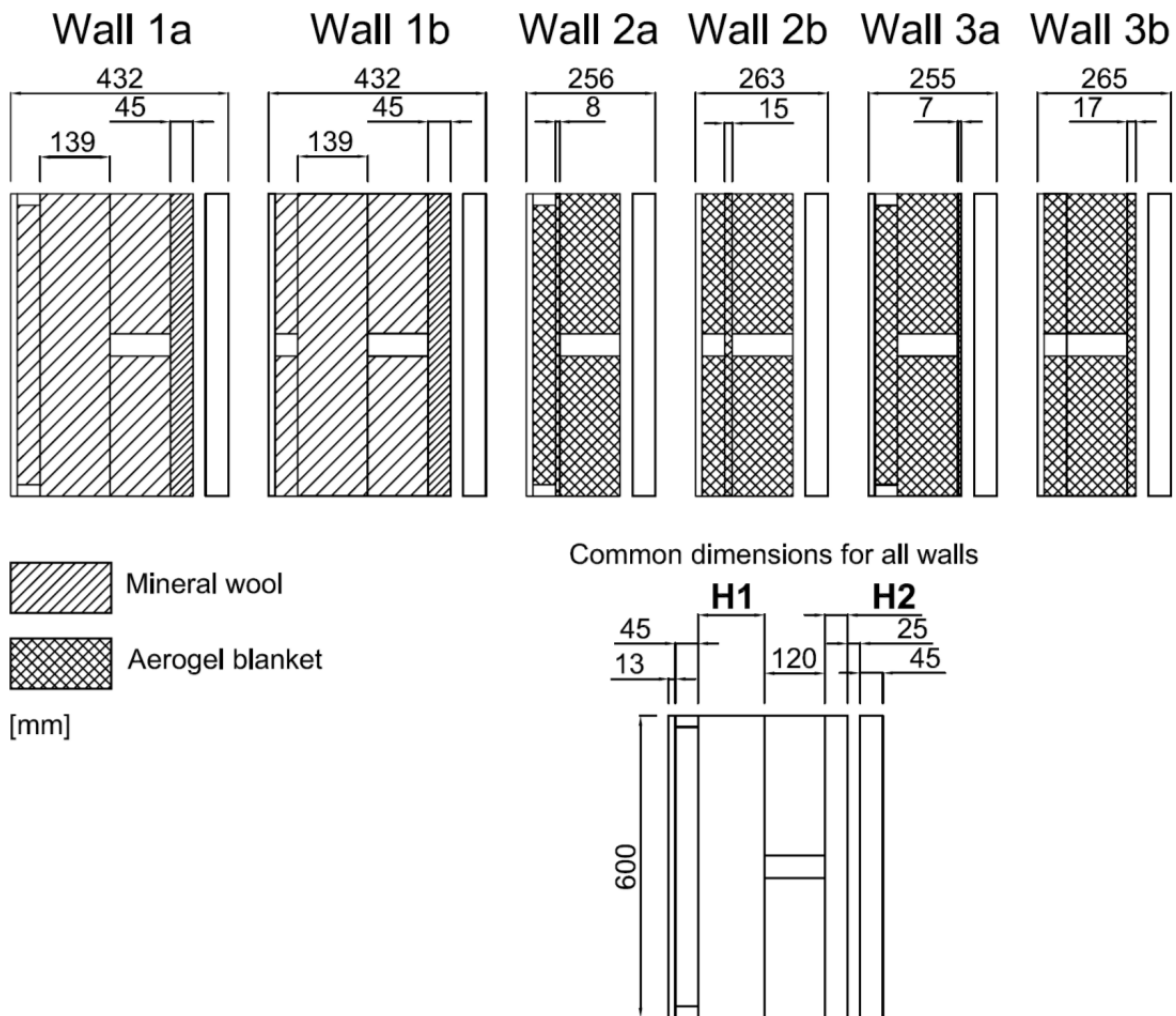


Figure 4.1 On top is horizontal incisions the six analyzed wall types with their different dimensions and in the bottom right is the common dimensions for all walls. The figure with the common dimensions also shows the location of the layers H1 and H2.

The thickness of the walls, required for the desired U-value, was determined by simulations in Comsol (2013), a finite element software, where heat flow through a wall at constant boundary temperatures was simulated. From the heat flow and the temperature difference, the U-value was obtained. The thickness of the layer H1 for wall 1a, 1b, 2a or H2 for wall 3a and 3b was adjusted until the U-value became 0.1  $W/m^2/K$ . The position of H1 and H2 are explained in the bottom right of Figure 4.1.

The thickness of the walls with aerogel was reduced by around 40 percent compared to the walls with mineral wool insulation. The thermal conductivity of the aerogel is less than half of the thermal conductivity of the mineral wool used in the calculations. This gives a theoretical possible thickness reduction by more than 50 percent. The difference from this theoretic value comes from the thermal bridges and the constant thickness of the façade and the interior plaster boards.

The moisture performance of the walls was analyzed in WUFI2D (2013), a coupled heat and moisture simulation software. The walls were exposed to a cycling of weather data from Göteborg, Sweden. The mold growth potential, defined as the quotient between the actual relative humidity and the critical relative humidity (Hukka & Viitanen, 1999), for each hour was calculated for the points shown in Figure 4.2.

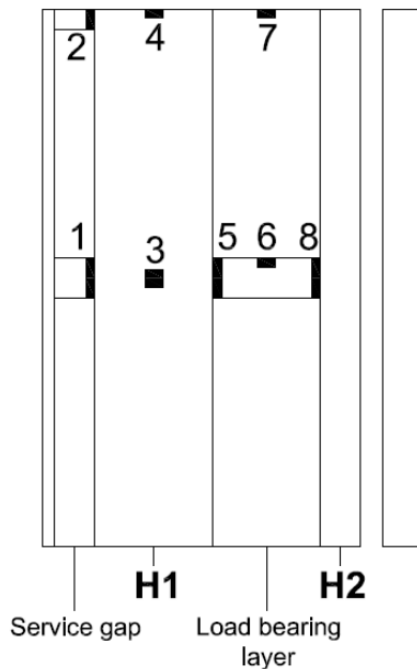


Figure 4.2 Position of the points for which the moisture conditions were evaluated.

The results for the maximum mold growth potential in each of the wall positions are shown in Figure 4.3. The best performing aerogel wall is 3b which gives results similar to the conventional walls in all points. Wall 2a and 2b, with the homogenous aerogel layer in the middle of the wall, gets very high mold potential in the load bearing studs which are exposed to conditions close to the outdoor climate. The results for wall 3a are similar to those of wall 3b in the outer construction of the wall but in the service penetration gap the mold potential exceeds 0.95. A mold growth potential at 0.95 is below the risk for started mold growth but a small variation in the moisture conditions could make it cross the limit.

The thermal bridge, created by putting the wooden studs of the load bearing structure and of the service gap in line, seems to be necessary to heat the structure at the position of the vapor tight film (position 1 and 2 in Figure 4.2) to prevent moisture problems on the inside of the film. This makes wall 3b the best performing aerogel wall from a moisture perspective, but at the same time it is the thickest of the aerogel walls.

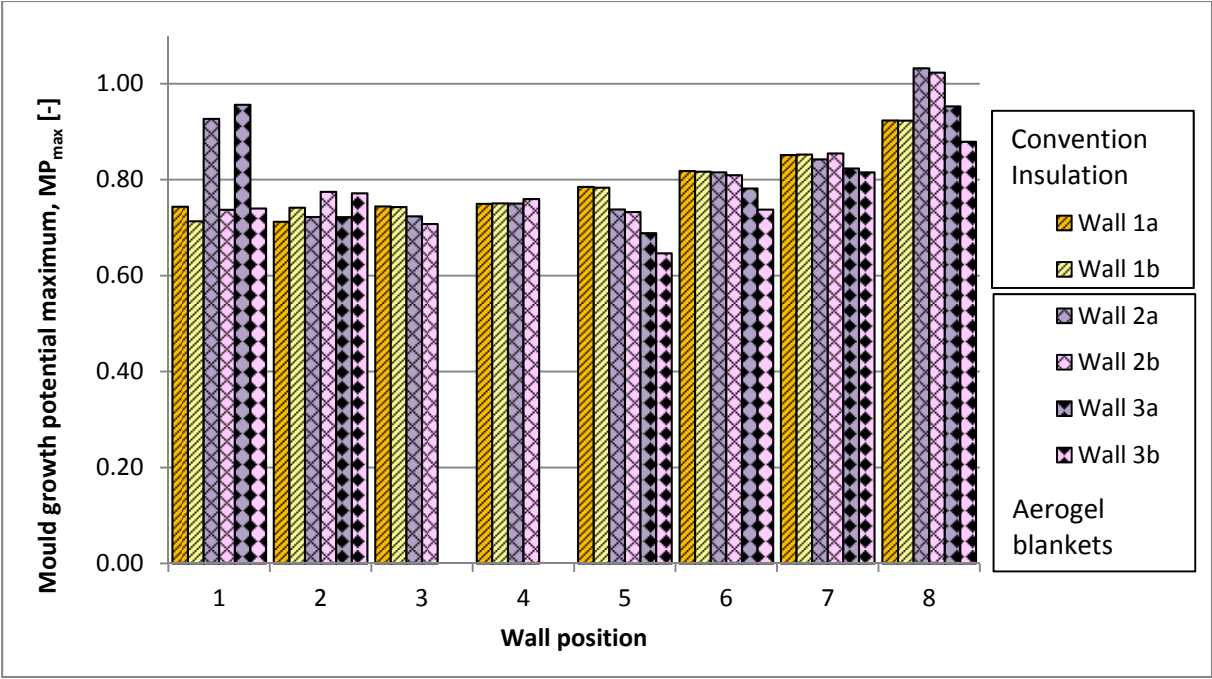


Figure 4.3 Maximum mold growth potential for each analyzed point in the walls.

## 5 Hybrid district heating pipes

Apart from external walls, the performance of aerogel blankets has also been investigated when used in district heating pipes. **Paper II** and **Report ii** investigate the application of novel insulation in district heating pipes. **Paper II** handles an early investigation of the possible benefits from superinsulation and some preliminary tests while **Report ii** investigates the performance of hybrid insulation district heating pipes more in detail.

Two concepts were developed and evaluated:

1. Blending aerogel particles with polyurethane to improve the thermal conductivity.
2. Adding a layer of superinsulation around the carrier pipe in the district heating pipe and filling up the rest of the cavities with polyurethane, explained in Figure 5.1.

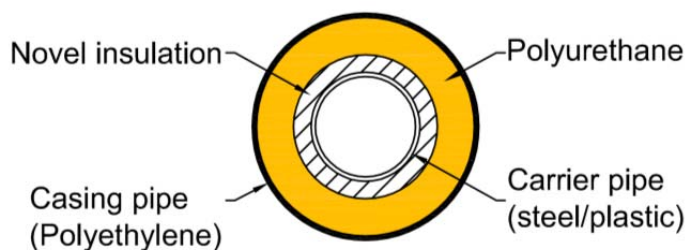


*Figure 5.1 The concept of the Hybrid insulation pipes with superinsulation around the carrier pipe and the rest of the pipe filled with polyurethane.*

The first concept, with blended aerogel particles, was evaluated by transient plane source measurements of the thermal conductivity. With a proportion between aerogel particles and polyurethane of around 7 percent and the mixing procedures used in these experiments, no improvement was detected when the thermal performance was compared to pure polyurethane. Therefore, this concept was put on hold and no more tests were performed.

The results for the layered concept showed more promising results why the tests were continued and this concept is the main focus of this chapter. The concept was used for a variety of pipe dimensions which are described by the nominal diameter (EN 10255:2004). As an example, DN 80/140 means a pipe with a carrier pipe diameter close to 80 mm and a casing pipe diameter of 140 mm.

### 5.1 Laboratory measurements

The investigations started by measurements of district heating pipes in the laboratory. The main focus was to evaluate the improvement in the thermal performance of district heating pipes with hybrid insulation.

#### 5.1.1 Guarded hot pipe

Measurements were performed with a guarded hot pipe apparatus. With the guarded hot pipe method, a one meter long specimen is placed in between two shorter guard segments with the same pipe dimension. A heating rod is inserted into the steel carrier pipe and the power to the rod is registered at the same time as the temperature on the inside of the pipe and the

temperature on the outside surface of the casing pipe. For a pipe with a homogenous insulation, this will give the value of the insulations thermal conductivity.

For the pipes with hybrid insulation, i.e. with varying layers of insulation, the method will give an apparent thermal conductivity which is linearly related to the heat loss at a specific temperature difference. Both district heating pipes with aerogel blankets and with vacuum insulation panels have been tested with the guarded hot pipe. The steel carrier pipes, enveloped by superinsulation, are shown in Figure 5.2, before the application of polyurethane.

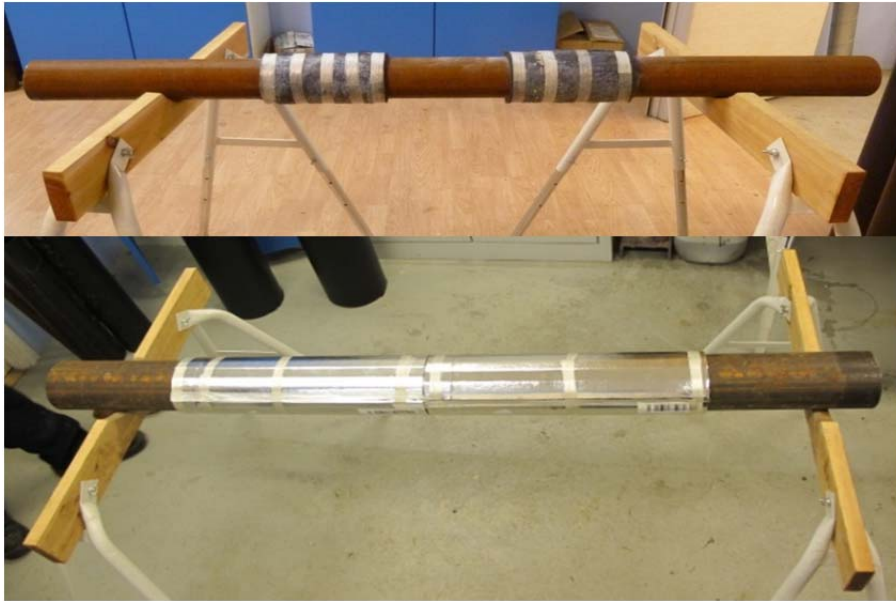


*Figure 5.2 The steel pipes of district heating pipes enveloped by aerogel blanket (above) and vacuum insulation panels (below). (Photo: Bijan Adl-Zarrabi)*

The results from the guarded hot pipe measurements are shown in Table 5.1 as apparent thermal conductivities, which is the calculated thermal conductivity of the whole hybrid set-up. The results shown in the table are mean values from two separate measurements. The results for the aerogel blanket pipes were calculated for the segments where the blanket was applied.

Table 5.1 Apparent conductivity of single pipes with superinsulation.

	Thickness of superinsulation [mm]	Apparent thermal conductivity at 50°C [mW/m/K]	Difference from Reference pipe [%]
<b>DN 80/140</b>			
Reference pipe <sup>1</sup>	0	28	0
Aerogel blanket <sup>1</sup>	10	23.7	-15
<b>DN 100/225</b>			
Reference pipe <sup>1</sup>	0	27.8	0
VIP <sup>1</sup>	5	23.5	-16
Reference <sup>2</sup>	0	26	0
VIP <sup>2</sup>	10	19.6	-33

<sup>1</sup> Polyurethane mixed in small scale

<sup>2</sup> Polyurethane mixed in product line

By calculating backwards from the resulting apparent thermal conductivity of the used polyurethane, the effective thermal conductivity of the layer with superinsulation can be found. Resulting effective thermal conductivities for the superinsulation layer, based on the apparent thermal conductivities in Table 5.1, can be seen in Table 5.2. The thickness of the insulation in the measurements is also shown since the thickness might have a large influence on the thermal bridges for vacuum insulation panels.

Table 5.2 Effective conductivity of superinsulation layers in district heating pipes. A typical value for the thermal conductivity of polyurethane is appended for comparison.

	Thickness of superinsulation [mm]	Effective thermal conductivity at 50°C [mW/m/K]
PUR	-	26.0
Aerogel blanket	10	16.5
VIP	5	11.4
VIP	10	10.3

The results showed a considerable decrease in heat losses. This gave incentives to make a more thorough investigation of the possibilities of the new materials. Since vacuum insulation panels gave largest decrease in the heat losses, further work focused mainly on these.

### 5.1.2 Field measurements preparations

To test the performance of the hybrid pipes during actual conditions, field measurements were prepared. The district heating grid, into which the measurement pipe would be connected, used double pipes, where the supply pipe and the return pipe are collected in the same casing pipe. In order to determine how to monitor the temperatures in double pipes in the field a special pipe sample was created to be analyzed in the guarded hot pipe apparatus. The sample

was a double pipe with the dimensions a carrier pipe diameter of 88.9 mm and a casing pipe diameter of 250 mm (DN 2\*80/250) and with a 10 mm vacuum insulation panel wrapped around half the length of the supply pipe, shown in Figure 5.3. Thermocouples were mounted inside the pipe before polyurethane was added

DN 2\*80/250 10mm VIP  
2011-11-9

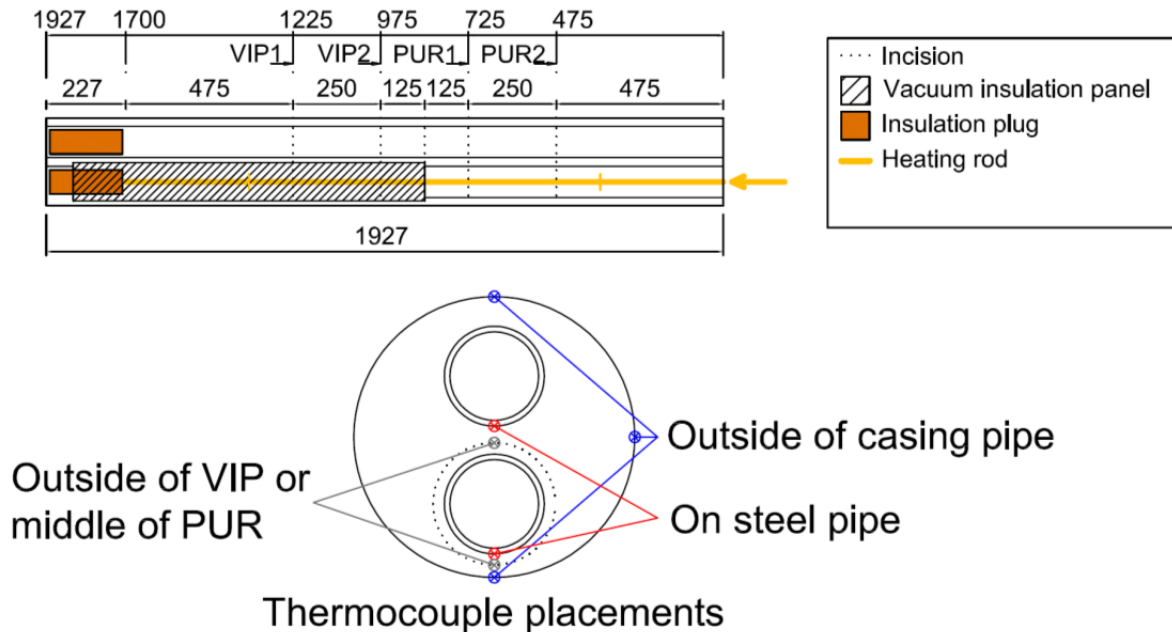


Figure 5.3 Description of the thermocouple placement in the preparation pipe to examine the possibilities of retrieving data from field measurements. The cuts in the steel pipe were made in incision A and the sensors are positioned in incision B1, B2, C1 and C4.

A heating rod was inserted into the supply pipe while the return pipe was left empty, but with sealed ends. The temperature was measured at various positions in the pipe. The temperatures in the half with only polyurethane was used as a reference to the results in the half with vacuum insulation. The measurements show that there was a clear difference in temperature in thermocouples mounted outside of the vacuum panel compared to the temperature of corresponding temperatures measured 10 mm out into the polyurethane, the same distance from the supply pipe as the outside of the vacuum panels. The measurements in the polyurethane differed a lot in between themselves, probably as a consequence of the method for positioning them in the middle of the polyurethane. Therefore, a more suitable method for thermocouple positioning was developed for field measurements.

The measurements also showed that the temperature of the steel pipes were the same independent on where the temperature was measured and thus, the steel pipe temperature could be used as a boundary condition.

## 5.2 Field measurements

Field measurements were performed to evaluate the long time performance of the vacuum insulation panels inside district heating pipes and are covered in **Report ii**. In January 2012 a district heating pipe with hybrid insulation were connected to the district heating grid. The pipe had the dimensions DN 2\*80/250 the measurement segment is shown in Figure 5.4. One half of the pipe is insulated with vacuum insulation panels while the other half is only insulated with polyurethane to work as a reference.

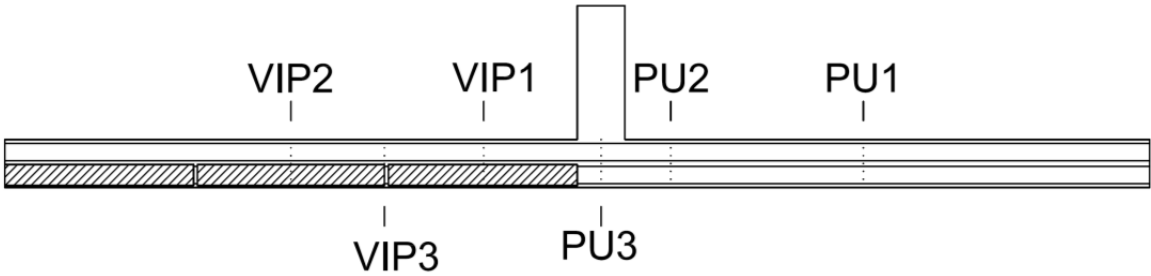


Figure 5.4 Measurement section of district heating pipe for field measurement. Temperatures were measured in the cross sections of VIP1 to 3 and PUR 1 to 3. In the middle of the pipe is a perpendicular pipe leading to the surface which holds the measurement equipment.

Thermocouples were mounted at different positions in the pipes and the temperature in the thermocouples have been registered every second hour since installment. The positions of the thermocouples are shown in Figure 5.5. The temperature is measured at similar positions in all cross sections shown in Figure 5.4. The two measurement positions furthest to the right in Figure 5.5 are related to the thermal bridges created by the permeation tight laminate that covers the vacuum insulation panels. The naming of the thermal bridges is defined in Figure 5.6.

	Supply: S	Return: R	Up: u-VIP	Side: s-VIP	Down: d-VIP	Thermal bridge along: TBA	Thermal bridge edge: TBE
	Supply: S	Return: R	Up: u-PUR	Side: s-PUR	Down: d-PUR	-	-

Figure 5.5 The naming of the measurement positions in the field measurements. The rows show positions in the part of the pipe with vacuum insulation panels (above) and in the reference part (below).

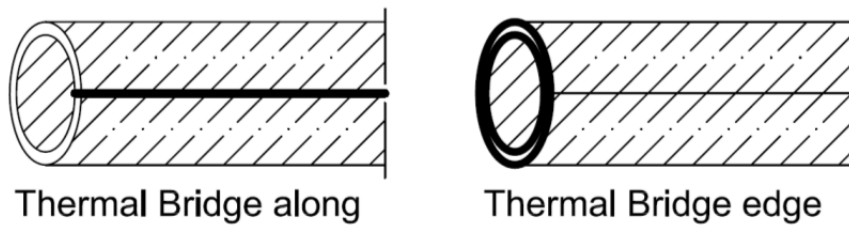


Figure 5.6 Explanation of the thermal bridges in the vacuum insulation panel. The thermal bridge to the left is called 'along the panel' and the thermal bridge to the right is called 'at the edge of panel'.

The measured temperatures are shown in Figure 5.7. The figure shows that the measurements in the same position follow the same pattern at similar temperature level. All the curves seem to react to the same changes in the temperature which can be seen in Figure 5.7 when the temperature changes quickly. This makes it appropriate to make a qualitative analysis on the mean value between various measurements in the same position. To make the figures easier to understand, the temperatures are also averaged over the weeks.

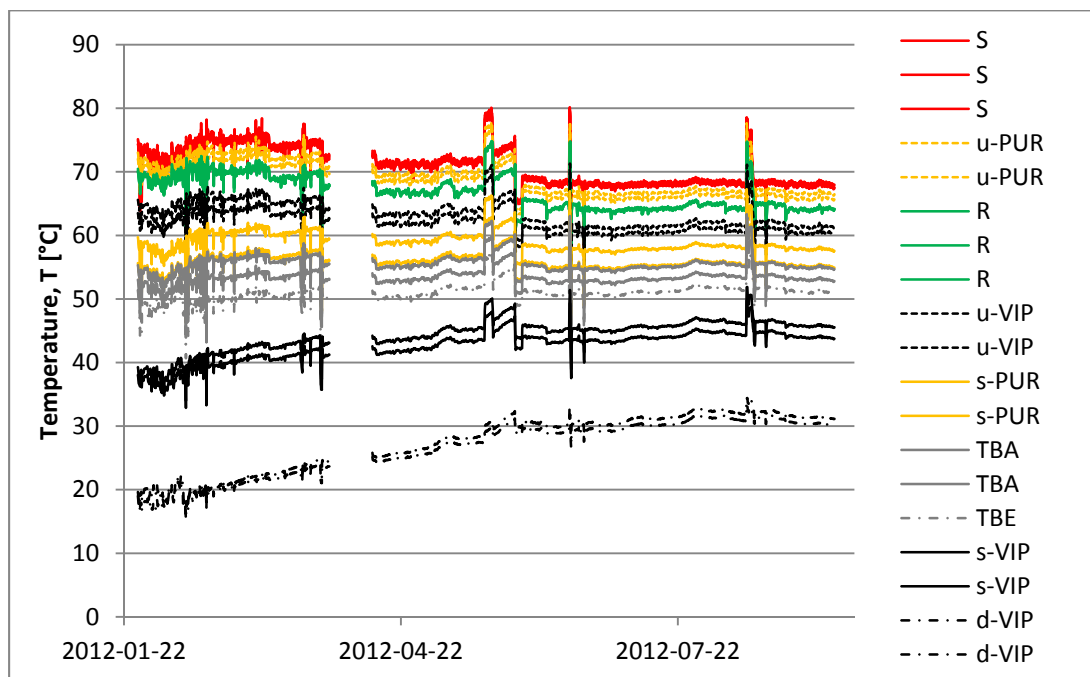


Figure 5.7 A collection of all temperature readings from the field measurements of double pipes connected to a district heating grid.

Figure 5.8 shows the temperatures on the side of the carrier pipe together with the supply (S) and return (R) temperatures for comparison. It is more than 10 °C difference between the temperature outside the vacuum insulation panel and inside the polyurethane at the same distance from the supply pipe. This means that the vacuum insulation panels work and have decreased the heat losses compared to the polyurethane. The temperature in the thermal

bridge is also lower than for the polyurethane which means that the flow is less even there, in the weakest point of the panels.

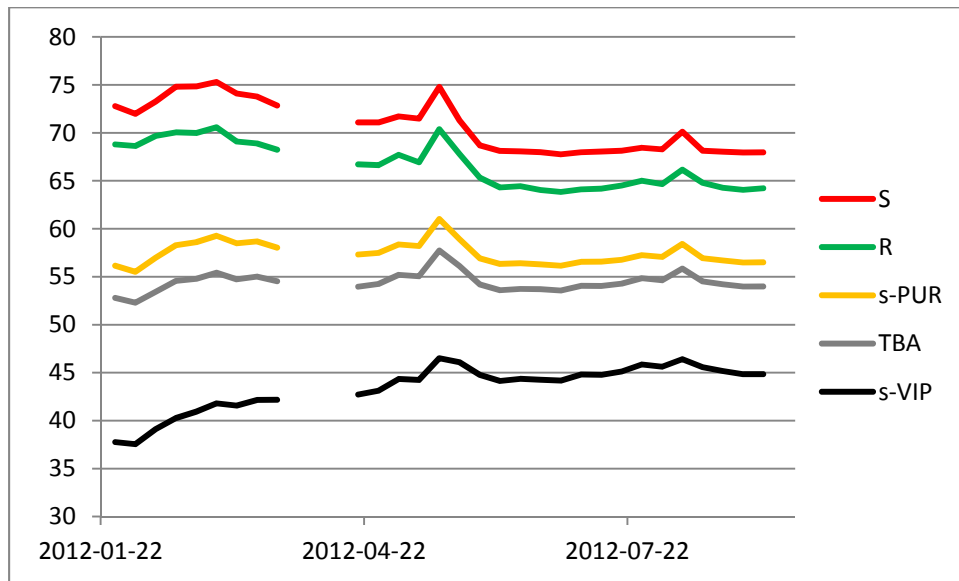


Figure 5.8 The mean temperature on the outside side of the vacuum insulation panel and the same position in the reference part together with the temperature in the supply and return pipe and on the thermal bridge along the vacuum insulation panel.

Another important factor is the durability of the vacuum insulation panels. Since the panels are placed in a high temperature environment inside the district heating pipe, the rate of air permeation into the panels will be increased compared to room temperature. It is also possible that the temperature will destroy the permeation tight laminate. The duration of the ongoing measurements have been too short to give any final conclusion on the durability of the vacuum insulation panels. Nevertheless, the results in Figure 5.8 show no temperature leaps which means that the vacuum insulation panels have not collapsed. The thermal properties of the vacuum panels are constantly deteriorating but the rate of the deterioration is too slow to be seen in these measurements.

## 5.3 Theoretical models

In order to evaluate the possible energetic benefit from using hybrid insulation in double pipes, the heat losses were calculated in **Report ii**. A numerical model was created and used to simulate the heat losses.

### 5.3.1 Description of numerical model

The finite element software Comsol (2013) was used to create the model for the double pipe in field. The model was created in two dimensions assuming constant conditions along the pipe. The input for the model is shown Figure 5.9.

An effective conductivity of 12 mW/(m·K) for the vacuum insulation panels, obtained from guarded hot pipe measurements, were used in the model. The polyurethane was given a

thermal conductivity of 26 mW/(m·K) at 50°C, which is a value obtained from the pipe producer.

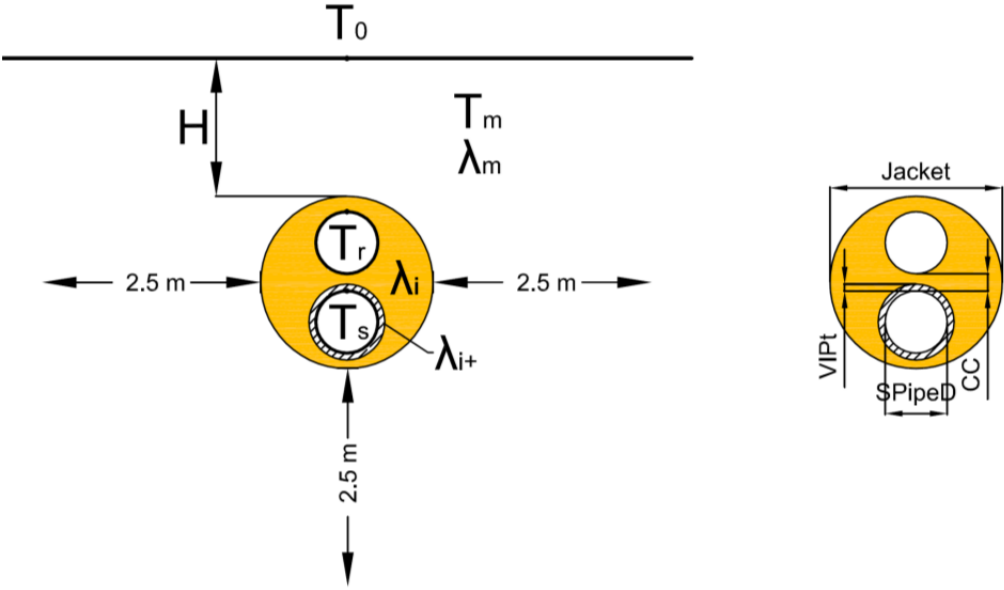


Figure 5.9 Input for the model of a double pipe in field. The figure to the left shows the needed properties of the all materials and the position of the pipe. The figure to the right show the input for the pipe dimensions.

### 5.3.2 Network model for arbitrary boundary conditions

To create results which were independent of the boundary conditions a network model was created shown in Figure 5.10. The heat flows were separated into three flows in between the three boundary temperatures; the supply pipe ( $T_s$ ), the return pipe ( $T_r$ ) and the ambient air temperature ( $T_a$ ). These flows were assumed to be linearly dependent on the temperature difference between the boundaries and could thus be calculated from the thermal conductances ( $K_{1g}$ ,  $K_{2g}$  and  $K_{12}$ ) as described in Equation (10) (Claesson & Hellstrom, 2011). The conductances were calculated by using the two cases shown in Figure 5.11. From the conductances, heat losses could be calculated from arbitrary or variable boundary conditions.

$$q = K \cdot \Delta T \tag{10}$$

where  $q$  is the heat flow ( $W/m^2$ ),  $K$  is the thermal conductance ( $W/(m^2 \cdot K)$ ) and  $\Delta T$  is the temperature difference (K or °C).

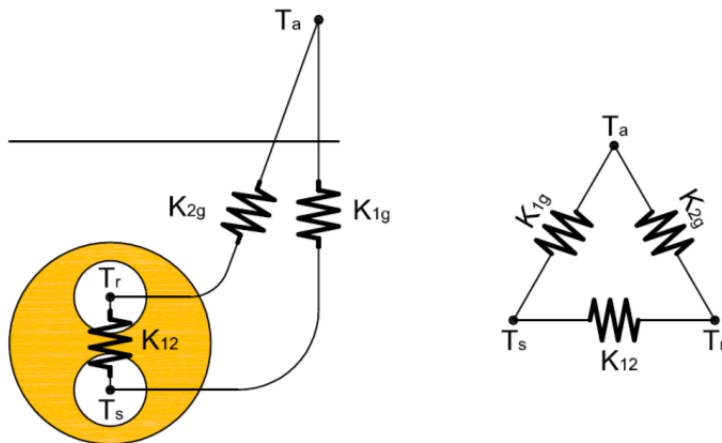


Figure 5.10 Thermal network describing linear heat flows in between the three boundaries; the supply pipe, the return pipe and the ambient temperature. To the right is a schematic image of the network and to the left is the network put in context.

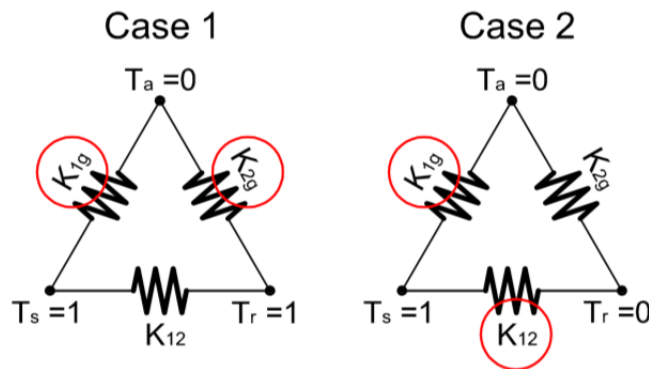


Figure 5.11 The two simulation cases which were used to calculate the conductances in the network shown in Figure 5.10.

### 5.3.3 Calculation of heat losses

To give an estimate of the heat losses from a pipe in field the conductances were calculated according to the two cases in Figure 5.11. The input data shown in Table 5.3 was used for the thermal properties

Table 5.3 Input data for the analysis of the heat losses from district heating pipes.

$\lambda_g$	Soil	1.5	W/(m·K)	
$\lambda_i$	Polyurethane	0.026	W/(m·K)	
$\lambda_{i+}$	Vacuum panel	0.012	W/(m·K)	
H	Depth	0.8	m	
$T_s$	Supply temperatur	85	°C	
$T_r$	Return temperatur	55	°C	
$T_a$	Ambient air temperature	5	°C	

The results for some various dimensions with alternating vacuum insulation thickness are shown in Table 5.4, both the conductances explained in Figure 5.10 and the heat loss from a

pipe with the boundary temperatures from Table 5.3 have been calculated. A layer of vacuum insulation seems to be able to lower the total heat losses out from the pipe to the ambient by around 15 to 25 percent compared to pure polyurethane, dependent on the dimensions of the district heating pipe and the thickness of vacuum insulation.

*Table 5.4 Resulting heat losses from numerical simulations of double pipes in the ground.*

	$K_{1g}$ W/(m·K)	$K_{2g}$ W/(m·K)	$K_{12}$ W/(m·K)	$Q_{out}$ W/m	$p_{Q_{out}}$ %
<b>DN 2*80/250</b>					
only PUR	0.182	0.184	0.078	23.76	0
1cm VIP	0.129	0.189	0.057	19.77	-17
<b>DN 2*80/280</b>					
only PUR	0.138	0.139	0.078	17.99	0
2cm VIP	0.089	0.144	0.046	14.32	-20
<b>DN 2*25/140</b>					
only PUR	0.102	0.102	0.049	13.26	0
1cm VIP	0.068	0.107	0.032	10.79	-19
1.5cm VIP	0.061	0.107	0.028	10.23	-23

### 5.3.4 Optimization of thermal bridge position

One simplification of the previous results is the use of the effective thermal conductivity of the vacuum insulation panel. This neglects the effect from the specific position of the thermal bridge through the metalized laminate.

The exact properties of the laminate is unknown but from the material producer we received an estimate in between 0.8 and 15 W/(m·K) along the laminate for a thickness of 0.1 mm. Both limiting conductivities were used to optimize the position of the thermal bridge along the panel. A numerical model of a single pipe was used to calculate the effective thermal conductivity of the vacuum panel if the thermal bridge along the panel was treated for. The model assumed constant temperatures around the casing pipe and in the steel pipe. Properties of the laminate were added into the model and the conductivity of the vacuum insulation panel was adjusted until the heat flow from the pipe corresponded to the measurements. This gave three different cases for the vacuum insulation panels listed in Table 5.5.

*Table 5.5 Effective thermal conductivity of the used vacuum insulation dependent on the thermal properties of the permeation tight laminate.*

	$d_{film}$ [mm]	$\lambda_{film,eff}$ W/(m·K)	$\lambda_{VIP,eff}$ W/(m·K)
VIP 1	0	0	0.012
VIP 2	0.1	0.8	0.012
VIP 3	0.1	15	0.010

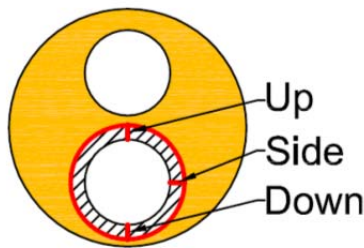


*Figure 5.12 The analyzed positions of the thermal bridge along the vacuum insulation panels.*

The results in Table 5.5 were used to optimize the position of the thermal bridge. Simulations were made with the thermal bridge in three different positions shown in Figure 5.12. The resulting losses are shown in Table 5.6 with the input data from Table 5.3 and Table 5.5.

The heat losses  $Q_{\text{out}}$  are the total losses from the supply pipe and the return pipe to the ambient temperature. The total heat losses show the energy loss from the whole system. The heat losses  $Q_{\text{supply}}$  are the heat losses from the supply pipe to the ambient temperature and to the return pipe. This is the heat losses from the system prior to reaching the customer. Dependent on the system for heating the district heating water, different loss terms might be relevant.

For most dimensions and thicknesses, an upward position of the thermal bridge gives the lowest losses both for the total losses and for the supply losses. From a heat loss perspective an upward orientation of the thermal bridge is thus an optimal placement.

Table 5.6 Results from the optimization of the position of the thermal bridge,  $TB_{pos}$ , along the panels.

	$TB_{pos}$	$Q_{out}$ W/m	$P_{Qout}$ %	$Q_{supply}$ W/m	$P_{Qsupply}$ %
<b>DN 2*80/250</b>					
only PUR	-	23.76	0	16.9	0
1cm o-VIP 1	-	19.77	-17	12.03	-29
1cm o-VIP 2	up	19.77	-17	12.15	-28
”	side	19.93	-16	12.19	-28
”	down	20.17	-15	12.43	-26
1cm o-VIP 3	up	19.44	<b>-18</b>	12.15	<b>-28</b>
”	side	20.29	-15	12.38	-27
”	down	22.47	-5	14.37	-15
<b>DN 2*80/280</b>					
only PUR	-	17.99	0	13.38	0
2cm o-VIP 1	-	14.32	-20	8.5	-36
2cm o-VIP 2	side	14.53	-19	8.69	-35
2cm o-VIP 3	up	14.13	<b>-21</b>	9.45	-29
”	side	15.25	-15	9.16	<b>-32</b>
”	down	16.84	-6	10.45	-22
<b>DN 2*25/140</b>					
only PUR	-	13.26	0	9.63	0
1cm o-VIP 1	-	10.79	-19	6.4	-34
1cm o-VIP 2	side	11.08	-16	6.67	-31
1cm o-VIP 3	up	11.45	<b>-14</b>	7.8	<b>-19</b>
”	side	12.48	-6	8.11	-16
”	down	13.51	2	8.81	-9
1.5cm o-VIP 1	-	10.23	-23	5.72	-41
1.5cm o-VIP 2	side	10.52	-21	5.99	-38
1.5cm o-VIP 3	up	11.08	<b>-16</b>	7.65	<b>-21</b>
”	side	12.46	-6	7.79	-19
”	down	14.23	7	9.07	-6

## 6 Conclusion

The aim of this thesis was to investigate the properties and possibilities of two types of novel thermal insulation; vacuum insulation panels and aerogel blankets. The presented work shows that these types of insulation can decrease the dimensions both for building envelopes and for district heating pipes. The increased cost from using the new materials could be balanced against the value of extra space, but the gain from superinsulation can also be possible architectonic values, comfort or other environmental benefits apart from energy saving. Although, when aerogel blankets and vacuum insulation panels are used in new applications, various considerations appear, which have to be investigated thoroughly.

### **Material properties**

For the aerogel blankets the compression has to be considered during thermal conductivity measurements since there is an obvious inhomogeneity between the surface layer and the core of the blanket. Since the aerogel has a lower thermal conductivity than air, the compression removes the air voids in the surface and decreases the thermal conductivity. Although, the overall heat flow through the aerogel blankets increases with the compression.

The aerogel blankets are vapor open with vapor diffusivity comparable to conventional open pore insulation as mineral wool.

The vacuum insulation panels used in the district heating pipes have to be measured as a part of a system since the impact from the thermal bridges along the edges will be influenced by the surrounding materials.

The transient plane source model created for heat capacity measurements underestimates the heat capacity of the sample material. This underestimation indicates a potential nonlinearity problem which could come from convection. The influence of convection can be removed by evacuating the measurement set-up.

### **Application of aerogel blankets in wooden stud walls**

Wooden stud walls with 120 mm wide load bearing studs, a service penetration gap and a U-value of  $0.100 \text{ W}/(\text{m}^2 \cdot \text{K})$  were tested both with aerogel blankets and mineral wool as insulation. The usage of aerogel blankets decreased the wall thickness of around 40 percent compared to when conventional insulation was used.

The position of the thermal bridges becomes important for the moisture performance of the aerogel blanket walls. The constructions have to be tested for moisture performance in order to determine a final design. The best performing wall in this study, from a moisture perspective, was one of the walls where the thermal bridges lined up in the worst way for thermal performance.

### **Application of hybrid insulation in district heating pipes**

Both aerogel blankets and vacuum insulation panels can be used to improve the thermal performance of district heating pipes. The actual improvement of the thermal performance depends on the dimensions of the pipes and on the superinsulation. A thickness of 10 mm aerogel gave a 13-18% decrease in apparent thermal conductivity, for a single pipe with a

carrier pipe diameter of 89 mm and a casing pipe diameter of 140 mm (DN 80/140). A 5 mm thick vacuum insulation panel gave a 16% decrease in apparent thermal conductivity, for a single pipe with a carrier pipe diameter of 114 mm and a casing pipe diameter of 225 mm (DN 100/225).

Measurements of a district heating pipe placed in field in a low temperature system did not show any fast decay or momentary collapse of the vacuum insulation panels' performance. Data have so far been collected from almost one year of measurements.

At this early stage, concerning the life time of district heating pipes, the vacuum insulation panels perform better than a reference section with only polyurethane. The thermal performance is improved, even where there are thermal bridges in the vacuum insulation panels.

Numerical simulations of district heating double pipes, where the supply pipe has been insulated by vacuum insulation panels, show a decrease in the heat losses of 15 to 25 percent compared to a pipe of the same dimensions with only polyurethane as insulation. The results depend on the dimensions of the pipes and the applied vacuum insulation thickness.

From heat loss perspective, the thermal bridge along a panel should be positioned upward, toward the return pipe. This minimizes both the heat losses during the transport of the thermal energy to the customer and the heat losses from the whole system. However, an upward position of the thermal bridge may generate problems with durability due to a higher temperature at the seams, and there might also be an inconvenience of upward thermal bridges when mass producing pipes.

## **7 Future studies**

The studies collected in this thesis make up a foundation for an understanding of the evaluation of aerogel blankets and vacuum insulation panels. This knowledge will be used for a more detailed analysis of new application concepts and also help to make good choices when measuring insulation properties.

The work will continue with measurements of more thermal properties and moisture properties of the aerogel blankets and vacuum insulation panels to create a sound foundation for assessment of application ideas.

More concepts for walls with superinsulation will be investigated. The problems and possibilities will be evaluated. The application concepts tested by simulations will be built and tested under real conditions.

The field measurements on hybrid insulation district heating pipes will continue in order to evaluate the long term performance of the vacuum insulation panels in a high temperature environment. The field measurements will also be used to validate the numerical model for double pipes in the ground. This will give a higher precision of the predicted heat losses so that a more detailed cost evaluation can be performed.

An analytical model for calculating the heat losses from hybrid insulation double pipes is under development and the work with the model will continue. It is possible that the analytical model can be simplified to get good estimates of the thermal performance from simple calculations without the need for simulation software.

The durability of the vacuum insulation panels at high temperatures will be further investigated to evaluate the thermal performance of hybrid pipes during their full service life. This is also a necessity for a calculation of the vacuum insulation panels payback time.

## 8 References

- Araki, K., Kamuto D. & Matsouka, S. (2009). Optimization about multilayer laminated film and getter device materials of vacuum insulation panels for using at high temperature. *Journal of Materials Processing Technology*. 209, pp. 271-282.
- ASPEN (2011a). *Aerogel Insulation Composite Improves U-Value of Barrel Vault Ceiling*. [www.aerogel.com](http://www.aerogel.com) > products > product case studies > building and construction [Available: 2013-03-18]
- ASPEN (2011b). *Aerogel Insulation Converts Old Mill House Into Modern Energy-Saving Passive House*. [www.aerogel.com](http://www.aerogel.com) > products > product case studies > building and construction [Available: 2013-03-18]
- ASPEN (2011c). *Aerogel Insulation Stops Thermal Bridging in Apartment Windows*. [www.aerogel.com](http://www.aerogel.com) > products > product case studies > building and construction [Available: 2013-03-18]
- ASPEN (2011d). *Wood Framing Insulated With Aerogel Improves Energy Efficiency by 15%*. [www.aerogel.com](http://www.aerogel.com) > products > product case studies > building and construction [Available: 2013-03-18]
- Baetens, R., Jelle, B.P. & Gustavsen, A. (2010). Aerogel insulation for building applications: A state-of-the-art review. *Energy and Buildings*, 43, pp.761-769.
- Binz, A., Moosmann, A., Steinke, G., Schonhardt, U., Fregnan, F., Simmler, H., Brunner, S., Ghazi, K., Bundi, R., Heinemann, U., Schwab, H., Cauberg, J. J. M., Tenpierik, M. J., Jóhannesson, G. A., Thorsell, T. I., Erb, M., and Nussbaumer, B. (2005). *Vacuum Insulation in the Building Sector. Systems and Applications (Subtask B)*: IEA/ECBCS Annex 39, High Performance Thermal Insulation (HiPTI).
- Claesson, J. & Hellstrom, G. (2011). Multipole method to calculate borehole thermal resistances in a borehole heat exchanger. *HVAC&R Research*. 17 (6) s. 895-911.
- Comsol. (2013) [www.comsol.com](http://www.comsol.com) [available: 2013-02-01].
- EN 10255:2004 (2004). *Non-alloy steel tubes suitable for welding and threading. Technical delivery conditions*. European committee for standardization.
- Eriksson, E. (2012) Praktiska tillämpningar av högpresterande värmeisolering i ombyggnadsprojekt. *Swedish Construction Industries organization for Research and Development (SBUF) project*. 12455.
- Fricke, J., Lu, X., Wang, P., Büttner, D. & Heinemann, U. (1992). Optimization of monolithic silica aerogel insulants. *International Journal of Heat and Mass Transfer*, 35(9), pp.2305–2309.

- Fuchsa, B., Hofbecka, K. & Faulstich M. (2012). Vacuum insulation panels – A promising solution for high insulated tanks. *Energy Procedia*. 30. pp.424 – 427.
- Haavi, T., Jelle, B.P. & Gustavsen, A. (2012). Vacuum insulation panels in wood frame wall constructions with different stud profiles. *Journal of Building Physics*, 36(2), pp.212–226.
- Hagentoft, C. (2001) *Introduction to building physics*. Lund, Sweden: Studentlitteratur. ISBN: 91-44-01896-7.
- Heinemann U. (2005). Influence of Water on the Total Heat Transfer in 'Evacuated' Insulations. *7th International Vacuum Insulation Symposium*. pp. 23-34.
- Hukka E. & Viitanen H. (1999) A mathematical model of mould growth on wooden material. *Wood Science and Technology* 33, Springer-Verlag.
- Hümmer, E., Rettelbach, T., Lu, X. & Fricke, J. (1993). Opacified silica aerogel. *Thermochimica Acta*, 218, pp.269–276.
- Kistler, S.S. (1931). Coherent expanded Aerogels. *Journal of Physical Chemistry*, 36(1), pp.52–64.
- Kubina, L. (2010). Etics with integrated vacuum insulation panels. *Proceedings of CESB10*, Prague, Czech Republic.
- Nilsson, O., Fransson, Å. & Sandberg, O. (1986). Thermal properties of silica aerogel. *Aerogels*. Springer Proceedings in Physics. Berlin: Springer-Verlag, pp. 121–132, ISBN: 3-540-16256-9.
- Parmenter, K.E. & Milstein, F. (1998). Mechanical properties of silica aerogels. *Journal of Non-Crystalline Solids*, 223(3), pp.179–189.
- Petersson, B.-Å. (2009). *Tillämpad byggnadsfysik* 3rd ed., Lund, Sweden: Studentlitteratur. ISBN: 978-91-44-05817-7.
- Pietruszka, B. & Gerylo, R. (2010). Implementation of nanoporous thermal insulations to improve the energy efficiency of curtain walling structures. *Proceedings of the 10th International Conference "Modern Building Materials, Structures and Techniques"*. pp. 255-258.
- Pietruszka, B., Babinska, J. & Gerylo, R. (2012). Aerogel-based thermal insulation materials - structure and properties. In *Proceedings of the 5th IBPC*. International Building Physics Conference. Kyoto, pp. 117–123.
- Reim, M., Körner, W., Manara, J., Korder, S., Arduini-Schuster, M., Ebert, H. & Fricke, J. (2005). Silica aerogel granulate material for thermal insulation and daylight. *Solar Energy*, 79, pp.131–139.

- Rubin, M. & Lampert, C.M. (1983). Transparent silica aerogels for window insulation. *Solar Energy Materials*, 7(4), pp.393–400.
- Simmler, H. & Brunner S. (2005). Aging and Service Life of VIP in Buildings. 7th International Vacuum Insulation Symposium. pp.15-22.
- Simmler, H. & Brunner S. (2008). In situ performance assessment of vacuum insulation panels in a flat roof construction. *Vacuum*, 82, pp.700-707.
- Simmler, H., Brunner, S., Heinemann, U., Schwab, H., Kumaran, K., Mukhopadhyaya, P., Quénard, D., Sallée, H., Noller, K., Küçükpinar-Niarchos, E., Stramm, C., Tenpierik, M. J., Cauberg, J. J. M., and Erb, M. (2005). *Vacuum Insulation Panels. Study on VIP-components and Panels for Service Life Prediction of VIP in Building Applications (Subtask A): IEA/ECBCS Annex 39 High Performance Thermal Insulation (HiPTI)*.
- Stahl, T., Brunner, S., Zimmermann, M. & Wakili, K.G. (2012). Thermo-hygric properties of a newly developed aerogel based insulation rendering for both exterior and interior applications. *Energy and Buildings*, 44, pp.114-117.
- STOAKES (2012). [www.stoakes.co.uk](http://www.stoakes.co.uk) > rooflights > Kalwall & Lumira Rooflights
- Sveipe, E., Jelle, B., Wegger, E., Uvsløkk, S., Grynning, S., Thue, J., Time, B. & Gustavsen, A. (2011). Improving thermal insulation of timber frame walls by retrofitting with vacuum insulation panels – experimental and theoretical investigations. *Journal of Building Physics*. 35(2). pp.168–188.
- Tamon, H., Sone, T. & Okazaki, M. (1997). Control of Mesoporous Structure of Silica Aerogel Prepared from TMOS. *Journal of Colloid and Interface Science*, 188(1), pp.162–167.
- Tillotson, T. & Hrubesh, L. (1992). Transparent Ultralow-density silica aerogels prepared by a two-step sol-gel process. *Journal of non-crystalline solids*, 145, pp.44–50.
- Va-q-tec (2013). [www.va-q-tec.com](http://www.va-q-tec.com) [available: 2013-05-08].
- Vip-bau (2013). [www.vip-bau.de](http://www.vip-bau.de) [available: 2013-05-08].
- WUFI 2D. (2013). [www.wufi.com](http://www.wufi.com) [available: 2013-02-01].